Advances in
Geo-Energy Research

Vol. 3, No. 3, p. 320-342, 2019
www.astp-agr.com

Invited review

A review on zeolitic imidazolate frameworks use for crude oil spills cleanup

Mozhgan Shahmirzaee[1], Abdolhossein Hemmati-Sarapardeh[1,2]*, Maen M. Husein[3], Mahin Schaffie[1,2], Mohammad Ranjbar[1,2]

[1]*Institute of Mineral Industries, Shahid Bahonar University of Kerman, Kerman, Iran*

[2]*Department of Petroleum Engineering, Shahid Bahonar University of Kerman, Kerman, Iran*

[3]*Department of Chemical & Petroleum Engineering, University of Calgary, Canada*

(Received July 9, 2019; revised July 22, 2019; accepted July 22; available online September 6, 2019)

Citation:
Shahmirzaee, M., Hemmati-Sarapardeh, A., Husein, M.M., Schaffie, M., Ranjbar, M. A review on zeolitic imidazolate frameworks use for crude oil spills cleanup. *Advances in Geo-Energy Research*, 2019, 3(3): 320-342, doi: 10.26804/ager.2019.03.10.

Corresponding author:
*E-mail: hemmati@uk.ac.ir

Keywords:
Zeolitic imidazolate frameworks
metal organic frameworks
oil spill
separation
pollution
water treatment

Abstract:
Oil spills are a global concern by virtue of their distractive effects on the ecosystem. Many studies have examined the use of porous materials as sorbents for contaminants from different polluted waters. For example, hydrophobic metal organic frameworks, especially zeolitic imidazolate frameworks (ZIFs) with high porosity, have attracted lots of attention. ZIFs are a subclass of metal organic frameworks and display an excellent performance toward oil/water separation compared with other porous materials. Nevertheless, the performance of ZIFs toward oil spills cleanup has not been reviewed. Accordingly, this article overviews the different methods for ZIF preparation, their corresponding structure, and their various applications as sorbents and in particular, recent developments in cleaning up oil spills with meso and micro-porous ZIFs. The investigation of the literatures revealed that the effective parameters on the performance of porous ZIFs are specific surface area, pore diameters of ZIF, and the size of cavities due to interconnecting of ZIF particles. The ZIF-8 with a high surface area of 1408 m^2/g and 1384.2 m^2/g and adsorption capacity up to 3000 mg/g was studied more than the other ZIF structures. Models predications revealed the maximum adsorption capacity of 6633 mg/g for ZIF-8. Recently, investigations focused on carbonitride foam and melamine sponge as templates of ZIF powder. In comparison with synthesis methods, dip coating as a facial synthesis method was introduced for production and anchoring ZIF particles on the substrate. The recyclability of crude oil and the reusability of the ZIF sorbents are highlighted. Moreover, this article reviews recent developments of ZIFs synthesis, current challenges, and prospects for the use of ZIFs in oil/water separation. The findings of this study can help to better understand widespread applications of ZIFs, effective features of a sorbent, and methods to improve adsorption capacity. As cleaning up oil spills is known as an important issue, this is the first study on ZIFs in particular oil/water separation which provides a summary of researches in a simple form along with recent developments compared to published reviews.

1. Introduction

Oil spills pertain to any intentional or accidental release of liquid hydrocarbons into the environment (Bhardwaj and Bhaskarwar, 2018). The industries such as oil production, refining, petrochemicals, plastics and metals produce oily wastewater which may find their way to different water bodies (Singh et al., 2011; Ge et al., 2014; Yu et al., 2015; Shi et al., 2016; Bhardwaj and Bhaskarwar, 2018; Yong et al., 2018). The ten largest oil spills in history have led to spilling millions of oil barrels into the seas as well as land regions. For example, about 240 to 336 million gallons of crude oil were spilled into the Persian Gulf in 1991, which marked the world largest oil spill. In 2010, 210 million gallons of oil were released from the British Petroleum (BP) platform over 3 months into the Gulf of Mexico. In June 1979, an oil well in Punjab Gulf suffered accidental explosion due to increased pressure, which led to the release of 140 million gallons to the Gulf of Mexico over 10 months. In order to reduce the oil spill from this incident, large quantities of sand, iron, and steel were injected into the main well. A summary of other oil spills between the years 1978∼2010 is provided in Table 1 (The Guardian Newspaper, 7 Oct 2011). One of the direct casualties can be named crippled by the accident of the tankers in the Caribbean Sea (1979) exploded in 300 nautical miles offshore, killing 26 crews.

https://doi.org/10.26804/ager.2019.03.10.

Table 1. The 10 biggest oil spills in the history (The Guardian Newspaper, 7 Oct 2011).

Number	Disaster region	Year	Oil spill
1	Persian gulf	1991	240 to 336 million gallons
2	Mexican Gulf	2010	210 million gallons
3	Mexican Gulf	1979	140 million gallons
4	Caribbean Sea	1979	88.3 million gallons
5	Uzbekistan	1992	87.7 million gallons
6	Persian gulf	1983	80 million gallons
7	Angola	1991	80 million gallons
8	South Africa (Saldanha Bay)	1983	78.5 million gallons
9	France (Brittany)	1978	68.7 million gallons
10	Canada (Nova Scotia)	1988	43 million gallons

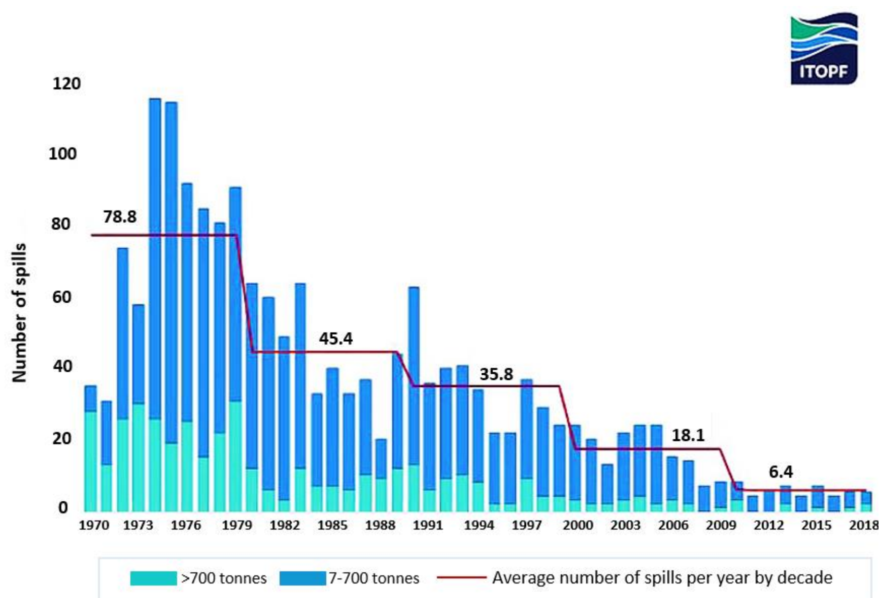

Fig. 1. Global oil spill trend from 1970 to 2018 (Reprinted with permission from ITOPF, 2019).

Other sources of water oil pollutants are wastewater from the industrial and transportation sectors (Kvenvolden and Cooper, 2003; Michel, 2011). Fig. 1 compiles oil spills based on the International Tanker Owners Pollution Federation (ITOPF) statistics from 1970 to 2018. These statistics suggest a significant reduction in the amount of oil spills, especially since 2010 (ITOPF, 2019). Distractive effects not only at the moment but also its consequences even 50 years after the incident are still being reported, nevertheless. Catastrophic effects on the marine environment, ecosystems and aquatics life, and quality of human life; including diseases and deaths is still a major challenge (Wu et al., 2014a; Jin et al., 2015; Jayaramulu et al., 2016; Guan et al., 2019).

Effective techniques for containing oil spills are well sought after. For example, spray, skinners, washing of surface were applied to remove oil spills from the sea. However, the seabed remained contaminated with the added substances (Fingas, 2011). Nanotechnology, on the other hand, is steadily advancing toward finding effective alternative materials which would minimize back contamination. Nanotechnology has been successfully employed in improving the performance of membranes, sorbents, magnetic materials, nanofibers, polymers, nanoporous structures, as well as carbon materials (Mokhatab et al., 2006; Lahann, 2008; Pendergast and Hoek, 2011; Shang et al., 2012; Xue et al., 2013; Zhang et al., 2013a; Gao et al., 2014; Kharisov et al., 2014; Si et al., 2015; Wang et al., 2015b; Wu et al., 2015; Lee et al., 2017; Fu et al., 2018; Gore et al., 2019). The membrane technology which has been developed for the separation and behaves as a porous medium has been studied theoretically and experimentally in two decades (Dejam et al., 2015a, 2015b; Dejam, 2018, 2019a, 2019b; Kou and Dejam, 2019). The higher demand for effective sorbents with less environmental impact led to the development of many porous structures with high surface area to mass ratio (Lin et al., 2012; Wu et al., 2012; Lei et al., 2013; Khosravi and Azizian, 2015; Bu et al., 2019; Shin et al., 2019;

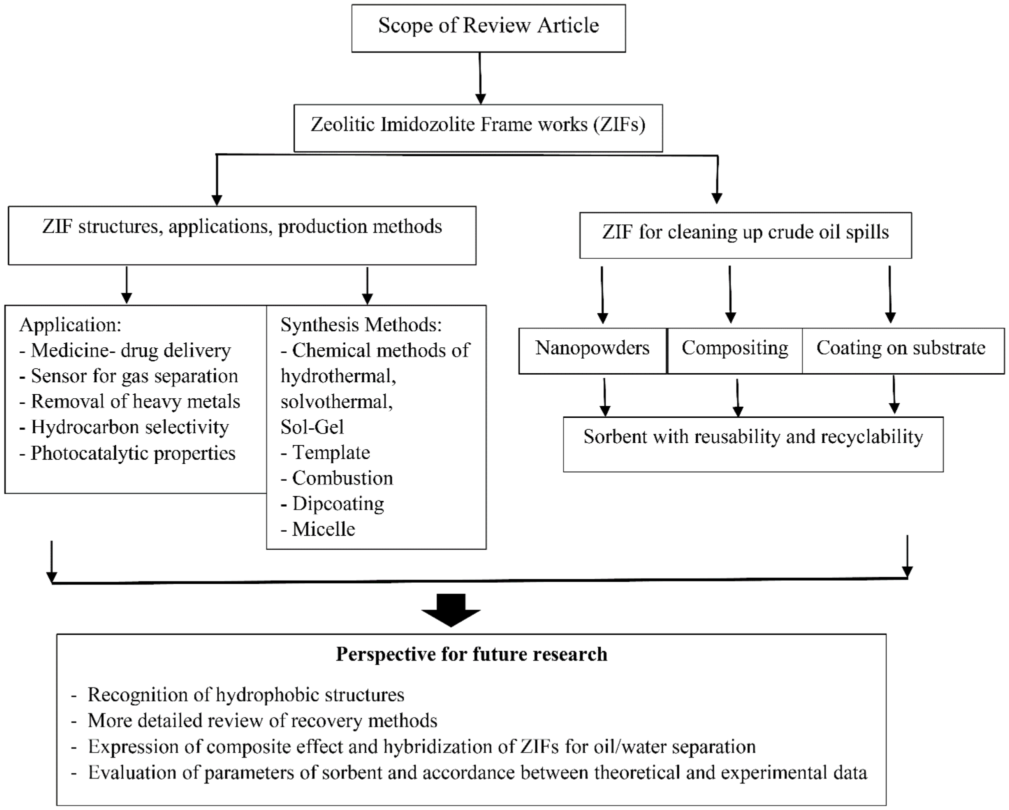

Fig. 2. Scope of review article for oil spills clean up.

Wang et al., 2019; Xu et al., 2019; Zhang et al., 2019b). Porous metal organic frameworks (MOFs) nanomaterials by virtue of their hierarchical porous structures, superhydrophobicity, rich functionalities, low cost, and suitability for large scale application have attracted attention in oil spill cleanup (Jayaramulu et al., 2017; Yoon et al., 2017; Gao et al., 2019; Kumar et al., 2019; Xu et al., 2019a, 2019b). Zeolitic imidazolate frameworks (ZIFs) are a group of MOFs. ZIFs with various structures have been used in many applications, especially crude oil spills due to hierarchical porous structures, facile synthesis, durability, and good recyclability (Seoane et al., 2011; Go et al., 2016; Wu et al., 2017a; Zhong et al., 2018). Based on predictive models, ZIFs absorption capacity is in the order of 6,600 mg/g (Lin et al., 2016).

The recent experimental studies have widely focused on oil/water separation as sorbent. In the published literature, ZIFs are reported as a novel sorbent in different shapes of powders, compositing with polymers, and coverage on a porous substrate or by their combination. The theoretical mechanism of oil/water separation depends on wettability, chemical composition, and surface structure introduced in theories of Wenzel (Wenzel, 1936) and Cassie-Baxter (Feng and Jiang, 2006). Polymers have been widely used in developing ZIFs which have become one of the powerful sorbents in oil/water separation. Polymers are used due to the flexibility and functionalization on the surface to change the wettability of active sites, and previous investigations confirm the effective presence of polymers. F-ZIF-90@PDA@sponge with loading PDA on the sponge surface increases the adsorption capacity up to 4800 wt% (Liu and Huang, 2018). More studies investigated various polymers such as ZIF-8/polymer composite beads with high adsorption capacity of 1,260 mg/g (Abbasi et al., 2017), ZIF-8 filled Polydimethylsiloxane for removal of n-Butanol from aqueous solution (Bai et al., 2013), ZIF-71/PDMS composite with high selectivity of alcohol from water (Yin et al., 2017), and so on. The modification of surface of the porous substrate was developed by compositing and ZIF-8 crystals coverage on the substrate. ZIF-8/CN foam is an example, in which wettability and surface roughness of carbonitride foam was modified by the attachment of ZIF-8 crystals and exhibited a high adsorption yield of 58 wt% (Kim et al., 2017). ZIF-8-melamine sponge composite increased the water contact angle up to 120° due to the contribution of ZIF-8 powders (Zhu et al., 2017). In this review, effective parameters of ZIF structures, pore volume, pore size, and adsorption factors on the capacity of ZIFs are explained. The scope of the review is shown in Fig. 2. Firstly, ZIF structures are described; then, various applications and synthesis methods are summarized in a table. Finally, ZIFs are described in different shapes of powder, composite with polymers and carbon materials, and in particular, ZIF as coverage on the substrate with a focus on sorbent for oil/water separation.

Compared to the other review articles, this study has investigated the popular ZIF literature from the first to 2019. This is a novel review which reports a group of sorbents compared to the review article (Bhardwaj and Bhaskarwar, 2018)

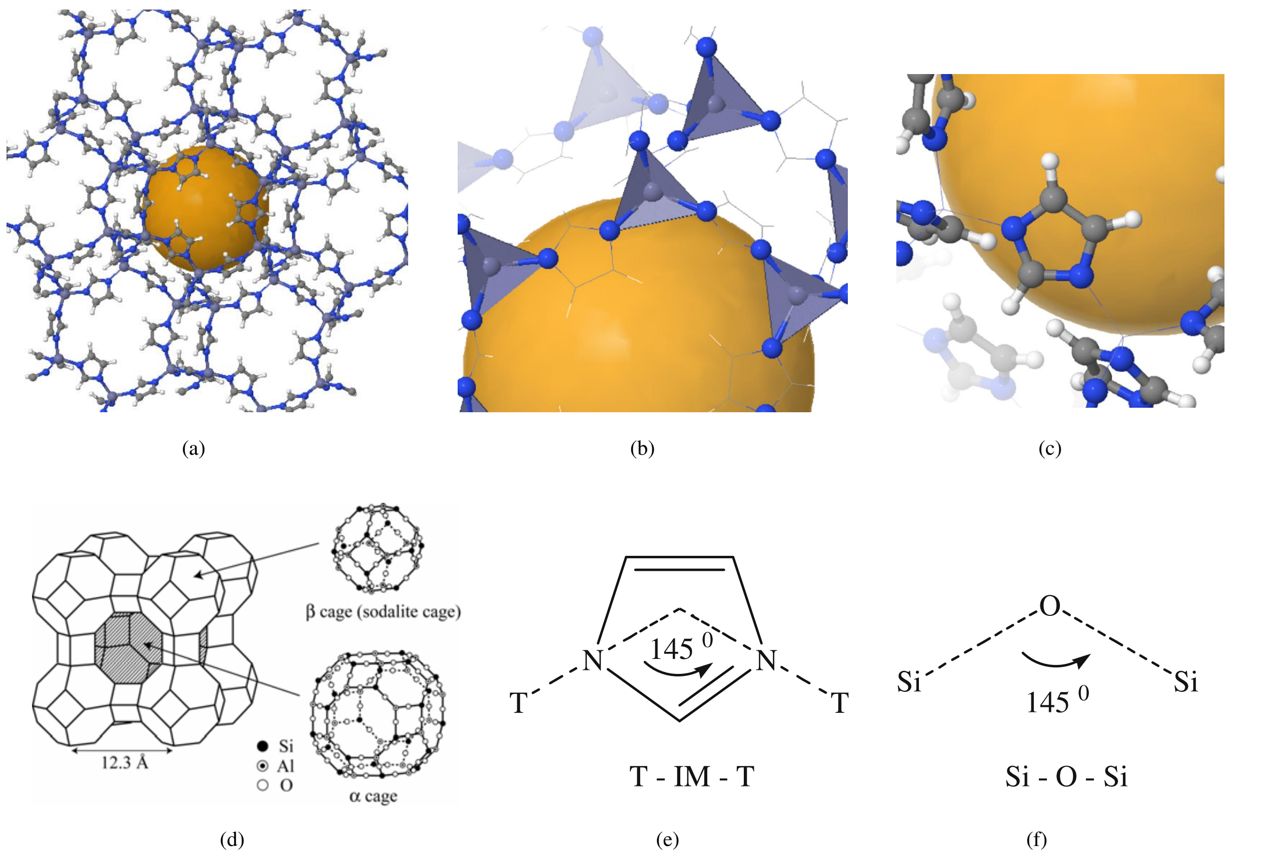

Fig. 3. (a) Zeolitic Imidazolate Framework (b) zinc ions (c) imidazolate rings (d) Aluminosilicate zeolite structure (e) Bond angle of ZIF structure (f) Bond angle of Zeolite (O-Si) (Nakano et al., 2007; Bhattacharjee et al., 2014).

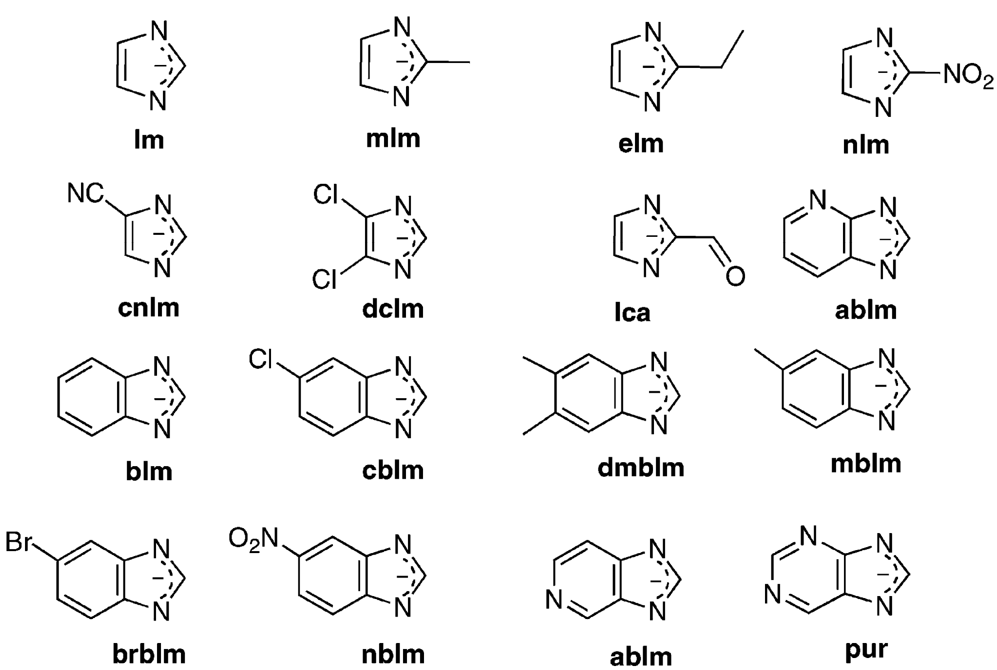

Fig. 4. Different types of imidazolate ligands (Phan et al., 2010).

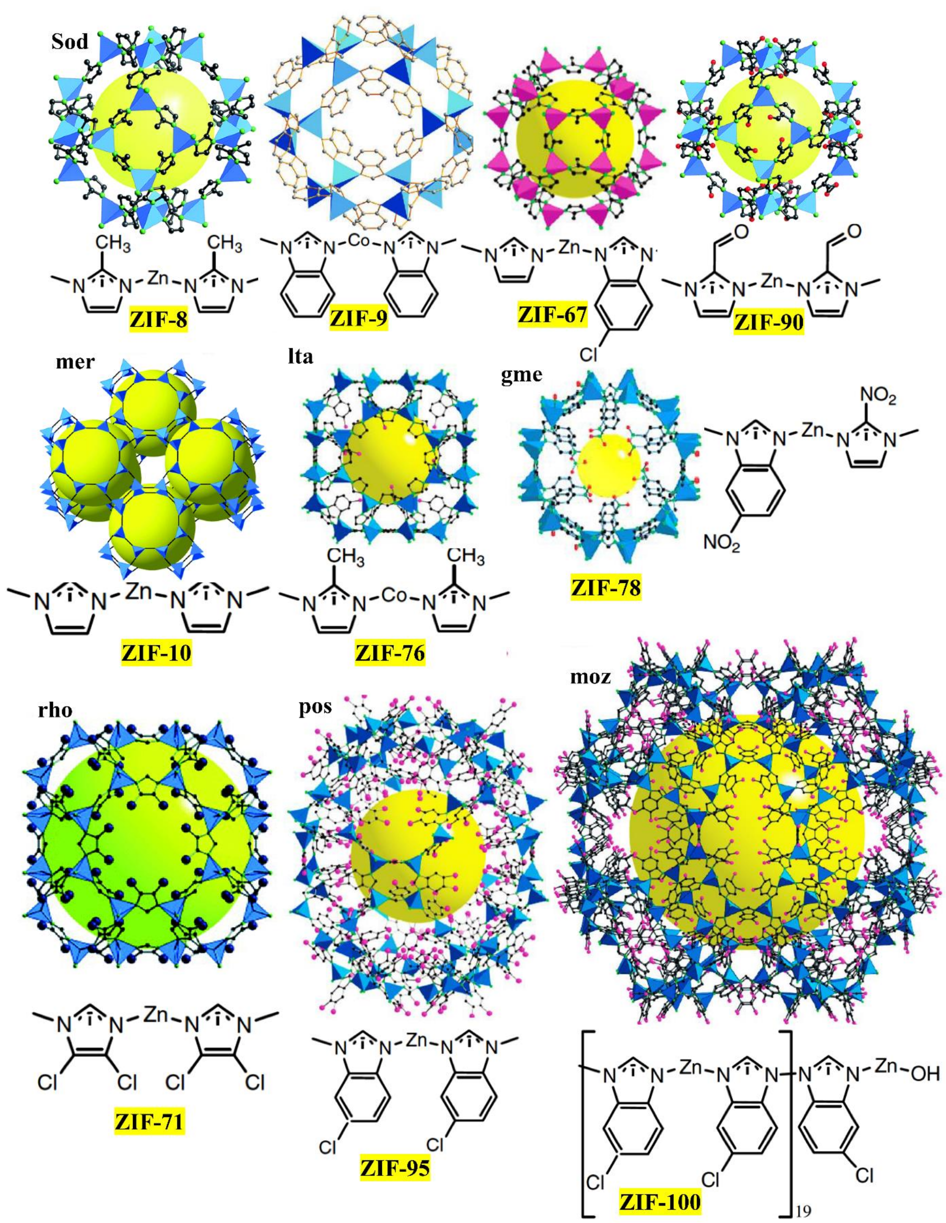

Fig. 5. Representative ZIF structures studied for catalysis/adsorption (Phan et al., 2010; Zakzeski et al., 2011).

that studied sorbents for oil-spill remediation but was not comprehensive on all of the sorbent examples. In addition, the sorbent structure, different shapes of structures, and the details of any factors such as wettability and adsorption capacity were not mentioned while this study shows them broadly. Another review of porous materials for oil/water separation introduced only a very few studies of ZIF sorbent (Guan et al., 2019). In other words, the review on porous materials described a small part of each sorbent role. Thus, this study on the ZIF sorbents provides a comprehensive survey which offers a good comparison between observations.

2. ZIF structures

ZIFs are a group of MOFs which are formed by organic imidazole as a ligand interconnecting the Zn in the tetrahedron structure of $Si(Al)O_4$ units in the zeolite as shown in Fig. 3 (Yaghi and Li, 1995; Xia et al., 2015; Lei et al., 2018; Liu and Huang, 2018), which have crystalline microporous of 1.16 nm ZIFs with bond angle of Zn-N are similar to Si-O in porous Zeolite material.

Fig. 4 presents the types of imidazole ligands and mixing of two imidazole structures (Phan et al., 2010). Some of the most common ZIFs are shown in Fig. 5, which are similar to standard zeolite with a topology, such as gme, sod, rho, lta, and ana. Other ZIF structures are summarized in Table 2, and experimental and theoretical studies keep adding more structures to the list. Different bonding and structural combination revealed pore sizes ranging from 1.6-19 Å and specific surface areas ranging from 620-2,800 m^2/g. The most important features of this novel material rely on symmetry

Table 2. The ZIFs discovered by high-throughput synthesis (Banerjee et al., 2008).

ZIF-n	Composition	Net (18)	ZIF-n	Composition	Net (18)
2	$Zn(IM)_2$	crb	62	$Zn(IM)_{1.75}(bIM)_{0.25}$	cag
3	$Zn(IM)_2$	dft	64	$Zn(IM)_2$	crb
4	$Zn(IM)_2$	cag	65	$Co(nIM)_2$	sod
8	$Zn(mIM)_2$	sod	67	$Co(mIM)_2$	sod
10	$Zn(IM)_2$	mer	68	Zn(bIM)(nIM)	gme
11	$Zn(bIM)_2$	rho	69	Zn(cbIM)(nIM)	gme
12	$Co(bIM)_2$	rho	70	$Zn(Im)_{1.13}(nIM)_{0.8}$	gme
14	$Zn(eIM)_2$	ana	71	$Zn(dcIM)_2$	rho
20	$Zn(Pur)_2$	lta	72	$Zn(dcIM)_2$	lcs
21	$Co(Pur)_2$	lta	73	$Zn(nIM)_{1.74}(mbIM)_{0.26}$	frl
23	$Zn(abIM)_2$	dia	74	Zn(nIM)(mbIM)	gis
60	$Zn(IM)_{1.5}(mIM)_{0.55}$	mer	75	Co(nIM)(mbIM)	gis
61	Zn(IM)(mIM)	zni	76	Zn(IM)(cbIM)	lta
			77	Zn(nIM)	frl

with hierarchical pores. Many new zeolite-like compounds have been discovered; however, with limited performance due to the lack of these main features (Rettig et al., 1999; Tian et al., 2002).

3. Summary of ZIF synthesis and applications

ZIFs with a hierarchical porous structure, large specific surface area, low cost of production, having exceptional thermal durability, and chemical stability (Kumar et al., 2014; Zheng et al., 2016) are promising candidates for various applications. The most common applications include catalysis (Yang et al., 2012; Kuruppathparambil et al., 2016), gas separation (Huang et al., 2012b), water purification from dyes (Guo et al., 2016), batteries (Huang et al., 2015), sensors (Lu and Hupp, 2010), proton conductor (Hurd et al., 2009; Taylor et al., 2010), heavy metal removal (Bo et al., 2018), biotechnology, and encapsulation (Liang et al., 2016a, 2016b). Table 3 summarizes the recent developments in ZIF preparation, composition, and application in the last two years. Table 4 presents an overview of ZIF applications and synthesis methods from 2008 to 2017. ZIFs are prepared using different techniques such as solvothermal (Zhang et al., 2019a), hydrothermal (Zhang et al., 2017; Yang et al., 2018), chemical solution (Shamsaei et al., 2016; Tsai and Langner, 2016), surfactant with dip-coating (Andrew Lin and Chang, 2015), coprecipitation (Wu et al., 2017b), sol-gel processing (Zhu et al., 2016), synthesis assisted template (Ren et al., 2019), silica aerogel (Shekhah et al., 2012), and pyrolysis (Ahmed et al., 2018). Investigations show that hydrothermal and solvothermal synthesis are common methods for ZIF production. Yuan et al. (2019) produced ZIF-300/α-Al_2O_3 membrane with a hydrothermal method, which showed porosity of about 35%. ZIF-300 crystals were heated at 120 °C for about 72 h in a hydrothermal process, and the membrane was produced using simple dip-coating route. ZIF-300 membrane exhibited 99.21% rejection of heavy metal ions and large water permeate flux, 39.2 L/m^2·h·bar. Another structure of ZIF having nanoscale hierarchically pores, ZIF-67 (NH-ZIF-67), was developed using a rapid process by employing an organic amine as a biofunctional modulator and accelerator of the nucleation (Li et al., 2019b). This study reflected high rates of adsorption of malachite green (MG) as well as high adsorption capacity of toluene. Wang et al. (2018a) fabricated LDH nano-flower using solvothermal method and ZIF-67 with the wet chemical route in methanol. ZIF-67 crystals showed great potential for organic adsorption from wastewaters. ZIF porous materials were also used for gas separation. ZIF-11 with a pore size of 36±6 nm exhibited H_2 and CO_2 adsorption with permeation values of 95.9 Barrer (Sánchez-Laínez et al., 2015). The centrifugation synthesis technique was applied between 1 and 30 min with molar composition initial materials of Zn: benzimidazole (bIm): NH_3: CH_3OH: toluene = 1: 2: 40: 300: 100 (Sánchez-Laínez et al., 2015). Firstly, solutions were cooled to 18 °C separately, and then, mixed in a centrifuge flask with 1,000 rpm. Composite studies of ZIFs, polymers, and carbon materials improved the performance of ZIF crystals. Barooah and Mandal (2019) reported PVA/PG/ZIF-8 membrane onto polyethersulfone (PES) support by methanol chemical route of coating for CO_2/N_2 gas separation with the yield of 98% higher than pure PVA/PG membrane.

Literatures have reported a widespread applications of core-shell ZIF. Miao et al. (2017) synthesized Fe_3O_4@P_4VP@ZIF-8 core-shell by a novel strategy of layer by layer, in which the microspheres were dispersed in 2-methylimidazole (2-MeIM) methanol solution. The core-shell structure portrayed efficient catalytic activity toward Knoevenagel condensation reaction. Zhang et al. (2018) reported a core-shell product, in which ZIF-L(Zn)@ZIF-67 nanoleaves were prepared by a chemical method as templates for coating hierarchically porous carbon materials. High specific surface area (359 m^2/g) of NC@GC(1)/CNTs and

Table 3. The most recent researches of ZIF applications (2018- 2019).

ZIF	Application	Synthesis method	Ref.
Methylene Blue@ZIF-8-reduced graphene oxide	Electrochemical sensing of rutin	Deposition	(Wang et al., 2018a)
ZIF-67/ Layered double hydroxides LDH	Adsorptive removal of organics from water	Solvothermal	(Wang et al., 2018b)
ZIF-8	Immobilizing Burkholderia cepacia Lipase for application in Biodiesel Preparation	Precipitation	(Adnan et al., 2018a)
ZIF-8	Adsorptive removal of sulfamethoxazole from water	Pyrolysis	(Ahmed et al., 2018)
ZIF-8	Encapsulation for Biodiesel Production-immobilizing Rhizomucor miehei lipase (RML)	Hydrothermal method	(Adnan et al., 2018b)
leaf-shaped zeolitic imidazo-late frame-work (2D ZIF-L)	Arsenite adsorbent	Aqueous solution-Precipitation	(Nasir et al., 2018)
Core-shell ZIF-L(Zn)@ZIF-67	Supercapacitor application	Chemical method	(Zhang et al., 2018)
ZIF-8	For monitoring the trace arsenic in fresh water	Micromixing system (novel)	(Parajuli et al., 2018)
Co-ZIF micro-structures on nickel foam	Glucose sensing and supercapacitor applications	Dip coating	(Arul and John, 2019)
ZIF-300	Membrane for removal of heavy metal Ions from wastewater with the water permeance of 39.2 $L/m^2 \cdot h \cdot bar$ and rejection rate of 99.21% for $CuSO_4$	Hydrothermal, Dipcoating	(Yuan et al., 2019)
ZIF-67 (NH-ZIF-67)	Adsorption performance with rate for capturing malachite green (MG) and higher adsorption capacity of toluene	Precipitation (novel)	(Li et al., 2019b)
PVA/PG/ZIF-8	CO_2 separation performance	Coating	(Barooah and Mandal, 2019)
ZnO@ZIF-8 core-shell	Ethanol gas sensing	Self-template method	(Ren et al., 2019)
ZIF-8/GO nanosheets	Amplified colorimetric detection of Ag^+	Precipitation and coating	(Li et al., 2019a)
ZIF-67 Nanoparticles in Hollow Carbon Nanospheres	Adsorption of CO_2	Nanospace confined synthesis	(Li et al., 2019c)
Fe_3O_4NPs@ZIF-8	Sensitive biosensing of organophosphate pesticides	Precipitation, encapsulated	(Bagheri et al., 2019)
Au@Ag nanorod@ZIF-8	Surface-enhanced Raman scattering imaging and drug delivery	Seed-mediated growth method	(Jiang et al., 2019a)
ZIF-90	Therapeutic outcomes of triple negative breast cancer in vivo	Self-assembly	(Jiang et al., 2019b)
Fe_3O_4@PAA@ZIF-8	Drug delivery of ciprofloxacin and investigation of antibacterial activity	Deposition	(Esfahanian et al., 2019)
Nafion/Hb/Au/ZIF-8/CILE	Electrochemical behavior of sensor for determination of bromate and nitrite	Deposition	(Liu, 2019)

Table 4. The history of researches of ZIF applications.

ZIF	Comments	Ref.
ZIF-68, ZIF-69, ZIF-70	Selectivity for CO_2 capture from CO_2/CO mixtures	(Banerjee et al., 2008)
ZIF-8	ZIF-8 on ceramic supports- membrane with Molecular Sieving Properties by Microwave-Assisted Solvothermal Synthesis	(Bux et al., 2009)
ZIF-8	Investigation of kinetic of separation of Propane and Propene	(Li et al., 2009)
Au@ZIF-8	ZIF-8 as a support for Au nanoparticles as heterogeneous catalyst	(Jiang et al., 2009)
ZIF-68 and ZIF-70	A simulation study (DFT) on adsorption and diffusion of light gases of CO_2, N_2, CH_4, and H_2. Simulations overpredict the amount of CO_2 adsorbed at 298 K compared with experiments	(Rankin et al., 2009)
ZIF-8	Applying pressure to ZIF-8 to 0.18 GPa to evaluate pore size changing	(Moggach et al., 2009)
ZIF-8	Membranes for CO_2/CH_4 Separation	(Venna and Carreon, 2010)

Table 4. The history of researches of ZIF applications (continued).

ZIF	Comments	Ref.
ZIF-68 and ZIF-69	Uptake and Selectivity of CO_2: strong Lewis acid-base interaction exists between the gas molecules and nitro groups of 2-nitroimidazole linkers, which thus prevents the entry of gas molecules into the small pores of ZIFs	(Hou and Li, 2010)
ZIF-69	Separation of CO_2/CO mixture. Membrane of porous -alumina substrate produced by solvothermal method and surface area of 1138m^2/g	(Liu et al., 2010)
ZIF-8 and ZIF-11	Simulation by molecular dynamics (MD) revealed symmetry independent adsorption sites of ZIF-8: above the imidazolate ring of C=C bond, adsorption sites of ZIF-11: top of the benzene ring	(Assfour et al., 2010)
ZIF-8	Catalysis of transesterification of vegetable oil. CO adsorption monitored by FTIR and DFT calculations (clusters and periodic models)	(Chizallet et al., 2010)
ZIF-90	Hydrogen selectivity from larger gases through 3-amino-propyltriethoxysilane as a covalent linker	(Huang et al., 2010)
ZIF-71	Ethanol uptake, water uptake significantly higher than model predictions	(Lively et al., 2011)
ZIF-90	Membrane for enhanced Hydrogen selectivity	(Huang and Caro, 2011)
ZIF-67	Gas adsorption and catalysis	(Qian et al., 2012)
ZIF-90	Membrane for gas-separation performance. Modification of ZIF-90: By covalent linkages between the free aldehyde groups of the ZIF-90 and the amino group of 3-aminopropyltriethoxysilane (APTES)	(Huang et al., 2012b)
ZIF-95	Membrane with cavities of 2.4 nm, for separation of H_2/CO_2, H_2/N_2,H_2/CH_4 and H_2/C_3H_8	(Huang et al., 2012a)
ZIF-11 and ZIF-7	Prediction using simulation MD and Monte Carlo schemes and transport theory, separation factors of 487 and 245 (H_2/N_2) for ZIF-11 and ZIF-7, respectively	(Thornton et al., 2012)
ZIF-8, -90 and -77	Natural gas purification (CO_2/CH_4)	(Thornton et al., 2012)
ZIF-8, -90 and -71	Air separation for oxy-combustion (O_2/N_2)	(Thornton et al., 2012)
ZIF-8	Drug Delivery Vehicle	(Sun et al., 2012)
ZIF-8	Development under hydrothermal conditions for adsorption and membrane separation	(Liu et al., 2013)
ZIF-8/PBI	Nano-composite membranes for high temperature hydrogen separation consisting of CO and water vapor	(Yang and Chung, 2013)
ZIF-90	ZIF-90 coating on silica fibers for the Solid-phase microextraction (SPME)	(Yu and Yan, 2013)
ZIF-8	Ethanol/Water Separation	(Zhang et al., 2013c)
Fe_3O_4@ZIF-8	Catalyst using magnetic properties	(Zhang et al., 2013d)
Zn-Fe-ZIF	Efficient oxygen reduction electrocatalysts	(Su et al., 2013)
ZIF-67	ZIF-67 as a template for synthesis of porous Co_3O_4. General applications in energy conversion and storage, catalysis, and drug delivery systems	(Wu et al., 2014b)
ZIF-67	Formaldehyde gas sensor in low concentration as 5 ppm in temperature of 150 °C with (surface area of 1832.2 m^2/g)	(Chen et al., 2014)
ZIF-8@GO	Membrane with Hydrogen selectivity. Separation factors of H_2/CO_2, H_2/N_2, H_2/CH_4, and H_2/C_3H_8 are 14.9, 90.5, 139.1, and 3816.6, with H_2 permeances of about 1.3×10^7 mol·m^2·s·Pa	(Huang et al., 2014)
Co-ZIF-9	Electrocatalyze the oxygen evolution reaction in a wide pH range: capable of activating the water molecule via binding the OH-group to the metal sites with low activation barriers	(Wang et al., 2014)
ZIF-8	Photocatalytic application	(Wee et al., 2014)
ZIF-11	Mixed matrix membranes for H_2/CO_2 separation	(Snchez-Lanez et al., 2015)
ZIF-8	Evolution using intrusion-extrusion of water under high pressure with energy yield varying from 80 to 93%	(Khay et al., 2015)
ZIF-11	H_2/CO_2 separation	(Snchez-Lanez et al., 2016)
ZIF-8	Membrane in Gas Separation	(Valadez Snchez et al., 2016)
CuS nanoparticles into the framework of ZIF-8	Synergistic chemo- and photothermal therapeutic effect on tumour cells	(Wang et al., 2016)
Fe_3O_4@P4VP@ZIF-8 Core-shell	Knoevenagel condensation reaction	(Miao et al., 2017)

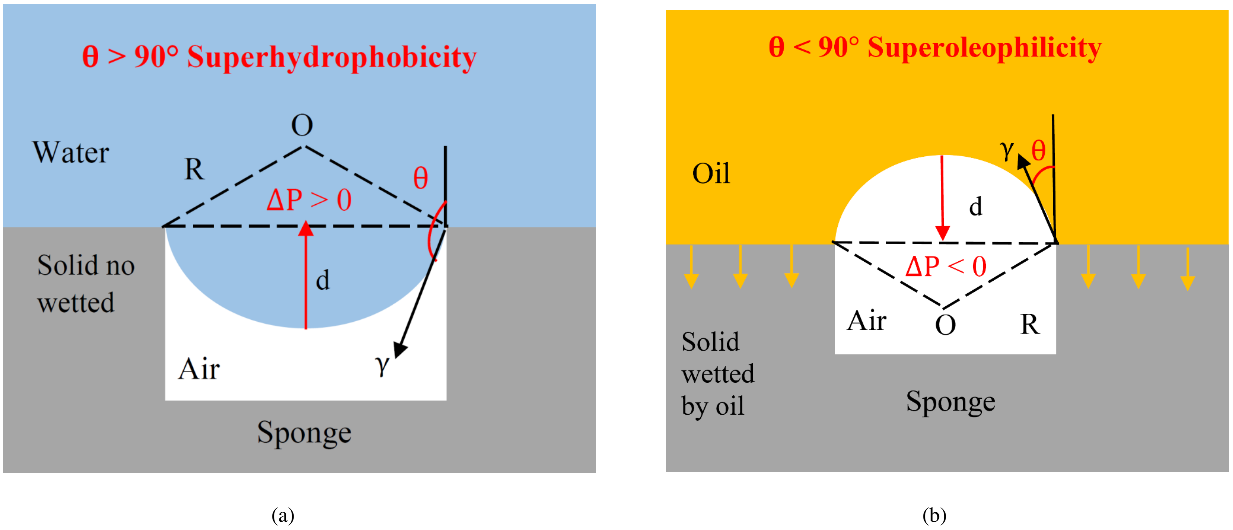

Fig. 6. Schematic of contact angle of water and oil for oil/water separation. (a) superhydrophobicity with $\theta_{A,water}>150°$, (b) superoleophilicity with $\theta_{oil}<90°$ (Tian et al., 2012; Wang et al., 2015a; Li et al., 2016).

N content (13.57 atomic%) were obtained. The electrical capacitance of the NC@GC(1)/CNTs, distinguished capacitance was very high, ∼(252.1 F/g), and the stability was exceptional, (∼91.2% capacitance retention following 10,000 cycle). This is a novel technique to extend the heterogeneous core-shell of ZIFs from different crystal structures. Medical applications were studied widely. ZIF-90 nanosystem with the self-assembling process was selected to synthesis DOX encapsulated nano ZIF-90. The research revealed ZIF-90 with better mitochondria targetability, cell biocompatibility, and in vivo survival rate than nano ZIF-8. It could be easily post-modified with Y1R ligand AP for active targeting drug delivery to TNBC cell line MDA-MB-231. The research in cancer diagnosis and treatment, explore the applicability of ZIF-90 in cancer treatment (Jiang et al., 2019b). Adnan et al. (2018) investigated ZIF-8 with X shape using encapsulation method and immobilizing Rhizomucor miehei lipase (RML) used for biodiesel production from soybean oil in an isooctane system with a conversion yield of 95.6%.

4. Sorption

Two main factors influence the sorption capacity of ZIFs; namely, their hydrophobicity and their specific surface area (Li et al., 2013; Nabeel Rashin et al., 2014). Wettability is assessed by the water contact angle (WCA). Fig. 6 shows how the contact angle is measured for porous materials. The pressure difference at the interface between oil/water and air in the porous medium is calculated by the Yong-Laplace equation (Eq. (1)) (Wang et al., 2015a; Li et al., 2016). Eq. (1) suggests intrusion pressure (Δp_{it}) in which γ, d, and R are interfacial tension of oil/water, the average of pore diameter, and sedi-diameter of the meniscus, respectively.

$$\Delta p_{it}=\frac{2\gamma}{R}=\frac{-4\gamma(cos\theta_A)}{d} \quad (1)$$

There are two types of intrusion pressure, negative and positive pressure. (a) $\theta_A< 90°$ and $\Delta p_{it}< 0$ where the oil penetrates to the pores by gravity, (b) $\theta_A> 90°$ and $\Delta p_{it}>0$, inert pressure is prevented from diffusing water (Zhang et al., 2015; Li et al., 2016). Meanwhile, for $\theta_{A,water}> 150°$, $\Delta p_{water}> 0$, or $\theta_{A,oil}< 30°$, oil intrusion pressure is $\Delta p_{oil}< 0$ as shown in Fig. 6. The oil penetrates through the porous media, easily but water is stopped from diffusion into the surface (Tian et al., 2012; Wang et al., 2015a; Li et al., 2016).

5. ZIF for oil/water separation

This review focuses on the ZIF crystals for hydrocarbon/oil-water separation. Studies on the application of ZIF materials for crude oil spills are summarized in Table 5 ZIF composition, water contact angle, surface area, and absorption capacity are shown with varied shapes of powder, coverage on template, and membrane.

The literature survey showed that ZIF-8 powder had demonstrated the high surface area of 1,408 and 1,384.2 m^2/g and adsorption capacity of 3,000 mg/g. Theoretical model predictions exhibit that the maximum adsorption capacity for ZIF-8 is about 6,633 mg/g (Lin et al., 2016; Sann et al., 2018). Therefore, it is an excellent candidate for oil/water separation, but the main problem is the removal of the sorbent at the end of the water treatment. ZIF-8 has been studied more than other ZIFs due to its thermal durability, chemical stability, strength and compatibility in composites. One of the main reasons for selecting the ZIF-8 is facile synthesis with 2-methylimidazole as ligand and no need to combine two or more ligands (Sann et al., 2018). Recently, researches have been progressing towards compositing and coating on a template. Investigations have revealed that polymeric and carbon materials are appropriate for compositing. ZIF/polymer composites such as PVDF-g-ZIF-8, PLA/ZIF-8 nanocomposite membrane, and F-ZIF-90@PDA@sponge illustrated water contact angle of 158°, 130°, and 159.1°, respectively. In addition, other ZIF structures such as ZIF-67, ZIF-71, and ZIF-90 were used in magnetic

Table 5. ZIF history for hydrocarbon/oil-water separation.

ZIF	Water contact angle, Surface area	Absorption capacity	Ref.
ZIF-8/polymer composite beads	115°, 1,030.6 m^2/g	1,260 mg/g	(Abbasi et al., 2017)
ZIF-8 powder	1,384.2 m^2/g	3,000 mg/g	(Lin et al., 2016)
ZIF-8@SiO_2@$MnFe_2O_4$	830 m^2/g	1,010.2 mg/g for MG and 78.12 mg/g for MO dyes	(Abdi et al., 2019)
F-ZIF-8@Kevlar	152.2°, 1.200 cm^3/g	Ethanol from water separation	(Li and Guo, 2018)
ZIF-8 Filled Polydimethylsiloxane	7.1 and 3.28×10^5 barrer	Removal of n-Butanol from aqueous solution	(Bai et al., 2013)
ZIF-8(Zn)/-67(Co)	576-1,050 m^2/g	10.4 mg/g of n-octane	(Bhadra et al., 2016)
ZIF-8/GO composite	967 m^2/g	n-octanol/water separation	(Bian et al., 2015)
ZIF-71/PDMS composite	Alcohol/water selectivity	Membrane for alcohol/water separation	(Yin et al., 2017)
Amine modification of ZIF-8	Membrane	Removal of Rhodamine B (RhB) and Methylene blue (MB) cationic dye	(Isanejad et al., 2017)
ZIF-8/reduced graphene-oxide aerogel	153°	Removal of oils and organic solvents	(Mao et al., 2017)
ZIF-67(Co)	1,259 m^2/g	260 mg/g, BTA and BZI removal from water	(Sarker et al., 2017)
ZIF-8(Zn)	969 m^2/g	260 mg/g, BTA and BZI removal from water	(Sarker et al., 2017)
Fe_3O_4-PSS@ZIF-67	491 m^2/g	52.50 mg/g nitrophenol from water	(Yang et al., 2018b)
graphene oxide/ZIF-67	491 m^2/g	Removal of cationic and anionic dyes from water, CV is 1,714.2 mg/g, for MO is 426.3 mg/g	(Yang et al., 2018a)
ZIF-8, ZIF-71 and ZIF-90	Membrane	Removal of alcohol (methanol, ethanol, 1-propanol, 2-propanol and 1-butanol)	(Zhang et al., 2013b)
MF-ZIF-8 sponge	140 °, 1,174 m^2/g	3,800 wt% for chloroform	(Lei et al., 2018)
ZIF-8-melamine sponge composite	120°	Absorption of organic solvents	(Zhu et al., 2017)
F-ZIF-90@PDA@sponge	159.1°, F-ZIF-90 is 690 m^2/g	1,600 wt% to 4,800 wt%	(Liu and Huang, 2018)
HFGO@ZIF-8	162°, 590 m^2/g	150-600 wt%	(Jayaramulu et al., 2016)
ZIF-8/polymer composite beads	115°, 1,030.6 m^2/g	1,260 mg/g	(Abbasi et al., 2017)
ZIF-8/CN foam	135°, 211 m^2/g	58 wt%	(Kim et al., 2017)
PLA/ZIF-8 Nanocomposite membrane	130°, ZIF-8 reaches 1185 m^2/g	Membrane for oil/water separation	(Dai et al., 2016)
ZIF-8 particles	142°, 1,408 m^2/g	70-250 wt%	(Sann et al., 2018)
PVDF-g-ZIF-8	158°	Separation yield of 92.93%	(Xu et al., 2018)

and polymer composites with larger cavities than ZIF-8. Lei et al. (2018) used a melamine sponge with a highly porous structure to construct the MF-ZIF-8 sponge composite to enhance hydrophobicity for the selective sorption of oil. First, polydopamine was doped on the melamine sponge template for structural modification to ensure powerful attachment of ZIF-8 powders. MF was immersed into dopamine with a solvothermal rout and formed a polymer film through polymerization and further deprotonation oxidation. Subsequently, it was placed into the precursor, including Zinc chloride and 2-Methylimidazole. The nucleation and growth of ZIF crystals were done during the solvothermal process (Figs. 7a-c). The water contact angle changed from 0° with micrometer-scale pores (50-200 μm) to an oleophilic structure. Various oil absorption capacities obtained from 1,000 wt% to the highest amount of 3,800 wt% for chloroform. It is powerful catalysis in the knoevenagel reaction. Figs. 7d-e shows absorbed and recovered oil by squeezing for further usage.

Zhu et al. (2017) reported ZIF-8-melamine sponge composite fabricated with acceptable mechanical properties by simple coating, which is cost-effective without complex equipment and easily scaled-up. A small cylindrical piece of sponge was immersed into a methanol solution having Zinc nitrite and 2-methylimidazolate for 1 h, and ZIF-8-melamine sponge was produced by washing and heating. As shown in Figs. 8b and 8c, a smooth skeleton was coated with a thin layer of ZIF-8 and confirmed the strength of about 13 kPa under compressive stress at 70% strain compared to brittle MOFs. In comparison with a hydrophilic sponge that water droplet penetrates its structure, ZIF-8-sponge showed higher hydrophobicity (water contact angle of 120°), where water drop stands on the sponge. The water contact angle did not change after 10 cycles (Fig. 8d).

Mondal et al. (2017) reported the synthesis of ZIF-

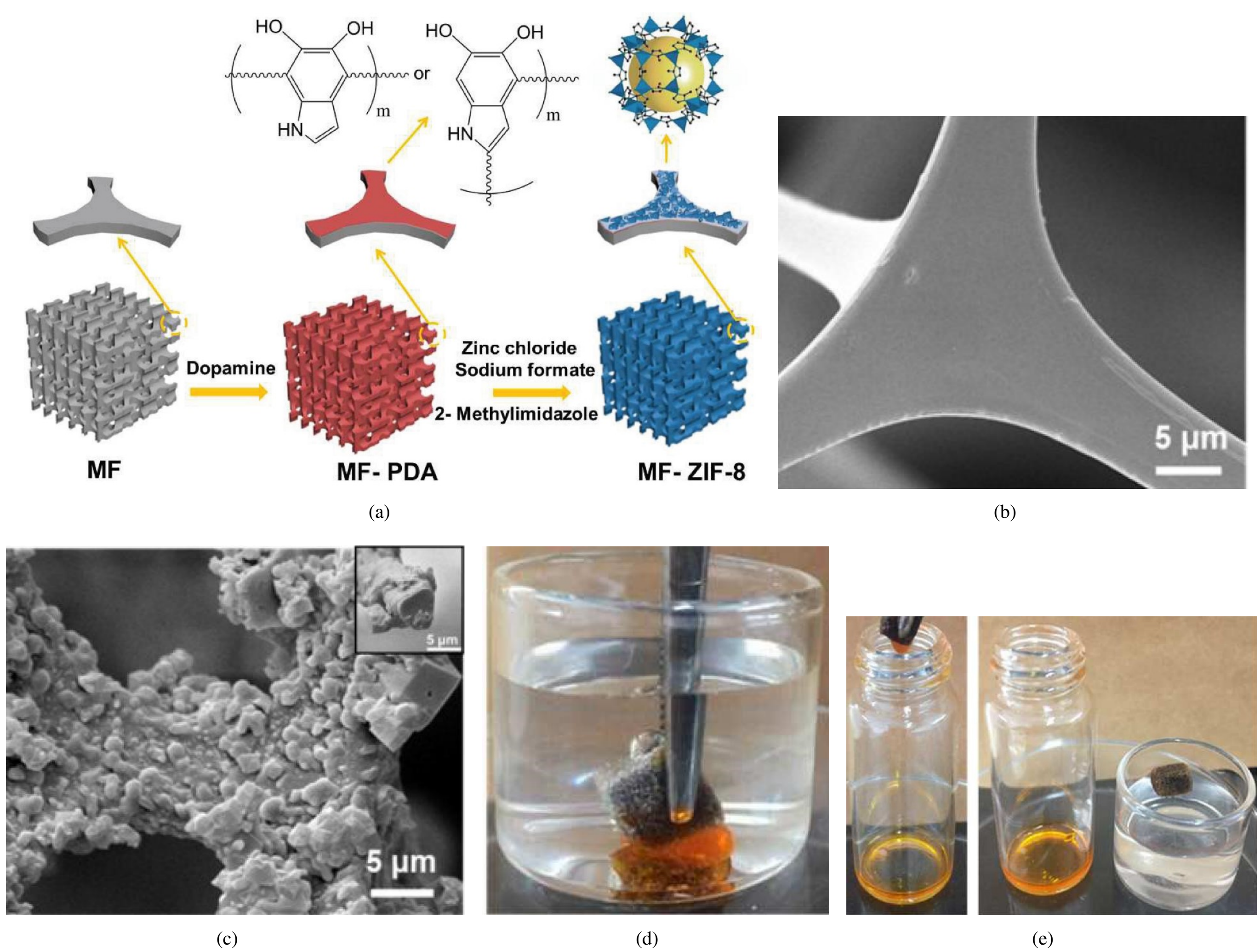

Fig. 7. (a) Schematic preparation of MF-ZIF-8 sponge, (b-c) SEM micrograph of initial MF and MF- ZIF-8, (d) water/oil separation and (e) recovery process of by squeezing (Lei et al., 2018).

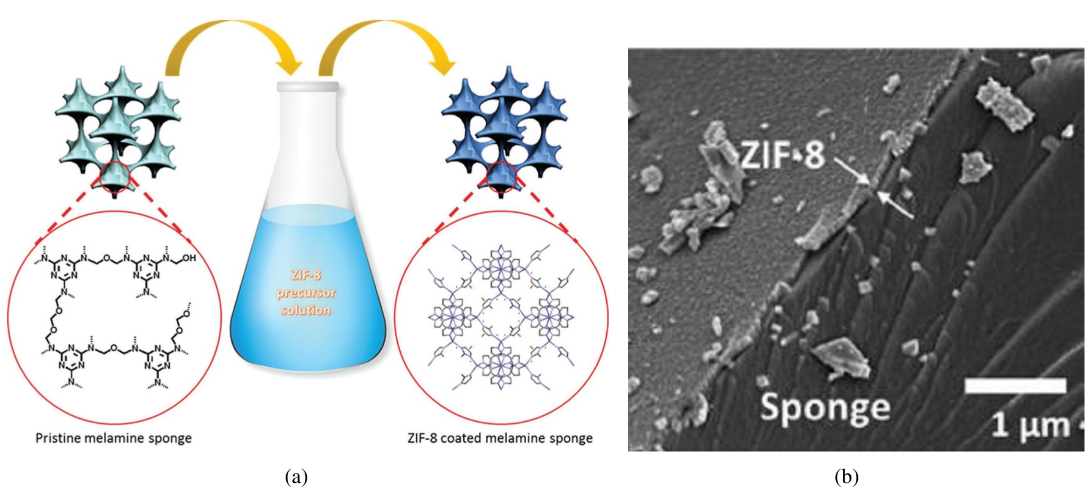

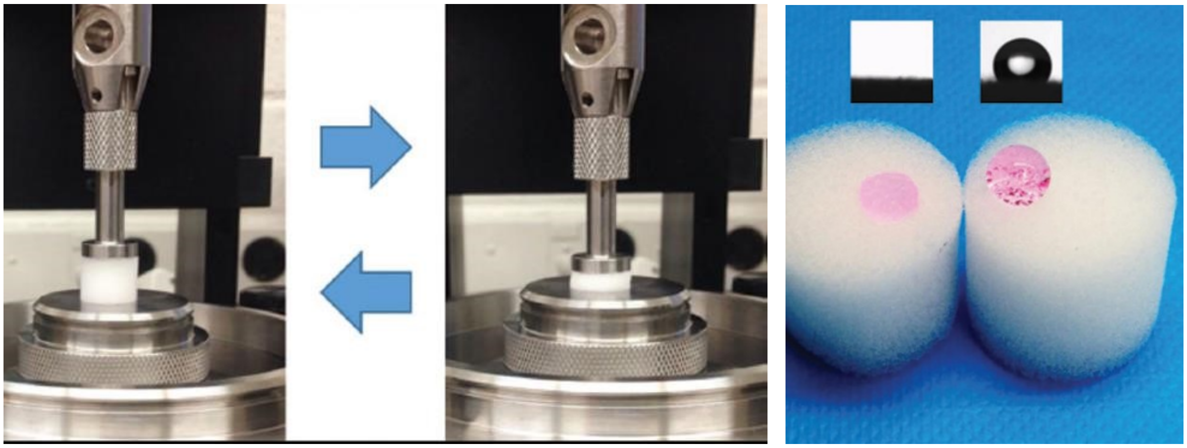

(c) (d)

Fig. 8. (a) Schematic preparation, (b) SEM micrograph of ZIF-8 coated melamine sponge, (c) compression test and (d) water contact angle of ZIF-8-sponge (Zhu et al., 2017).

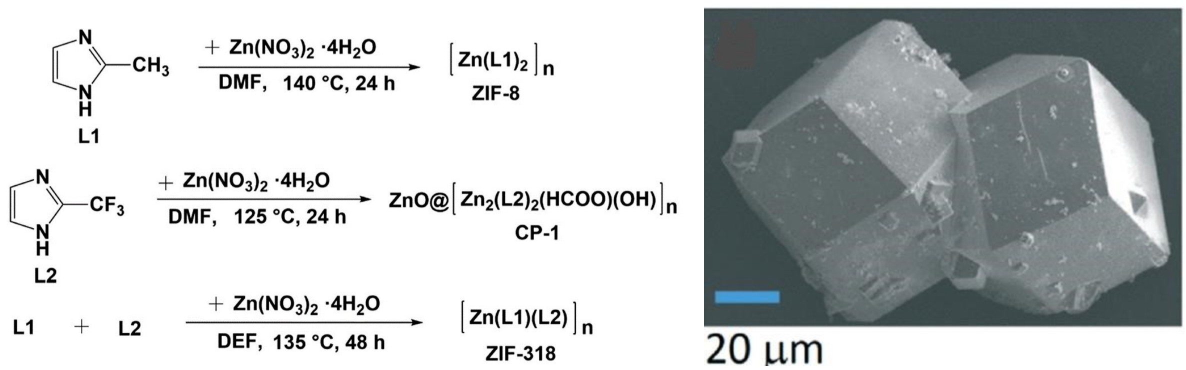

(a) (b)

Fig. 9. (a) Solvothermal synthesis, (b) SEM image of fluorinated ZIF-8 analog ZIF-318 (Mondal et al., 2017).

318 from the linkers of 2-methylimidazole (L1) and 2-trifluoromethylimidazole using the solvothermal method optimized for the separation of ethane/ethene mixtures (Fig. 9). This report modified the functionality of the imidazole linker. Replacement of -CH_3 with -CF_3 agent leads to a little change in the pore size and properties.

Based on the research of Liu and Huang (2018), F-ZIF-90@PDA@sponge composite was prepared using a fluorine-functionalized imidazolate as the organic linker. The polydopamine (PDA) was used to modify the surface of the sponge. Fluorine-functionalized imidazole-2-carboxyaldehyde (F-ICA) was prepared as an organic linker in two stages of solvothermal synthesis during the reaction of zinc(II) chloride, sodium formate, and F-ICA in methanol, separately (Fig. 10). The prepared sample showed high adsorption capacities for various oils and organic liquids ranging from 1,600 to 4,800 wt% for CCl_4 with the largest water contact angle of about 159.1°.

Jayaramulu et al. (2016) produced a highly fluorinated graphene oxide (HFGO)@ZIF-8, where ZIF-8 was connected at the graphene surface oxygen functionalities (Fig. 11a). This hierarchical structural architecture led to a superoleophilic behavior with the high water contact angle of 162° and low oil contact angle of 0° (Figs. 11b-c). Pore size was in the range of mesopores 1 nm and 3 nm for ZIF-8 structure and composite structure, respectively. The result of the absorption for various organic solvents was achieved 150-600 wt% for the maximum absorption of methanol.

Abbasi et al. (2017) studied the ZIF-8/polymer composite beads with polyethersulfone (PES) as a binder using the phase inversion synthesize method in the aqueous solution used in the research of Koji Kida et al. (Liang et al., 2012). Hydrophobicity and high surface area empower the composite for adsorption application. The diameter of ZIF-8 particles was about 250 nm and they have a very high surface area of 1,384.2 m^2/g BET and 1,849 m^2/g Langmuir surface area. Surface area values in different ZIF concentrations were obtained 343.2, 602, 882.3 and 1,030.6 m^2/g for ZIF/PES-0.5, ZIF/PES-1, ZIF/PES-2, and ZIF/PES-4, respectively. The highest adsorption capacity was related to ZIF/PES-4. The macro meter pore size distribution of PES spheres is shown in Fig. 12 with a water contact angle of 100° for the left and contact angle of 115° for the right.

Carbon nitride (CN) foams were employed to grow the crystalline ZIF-8 placed on N functionalities of CN with chemical anchoring (Fig. 13). The synthesis process includes

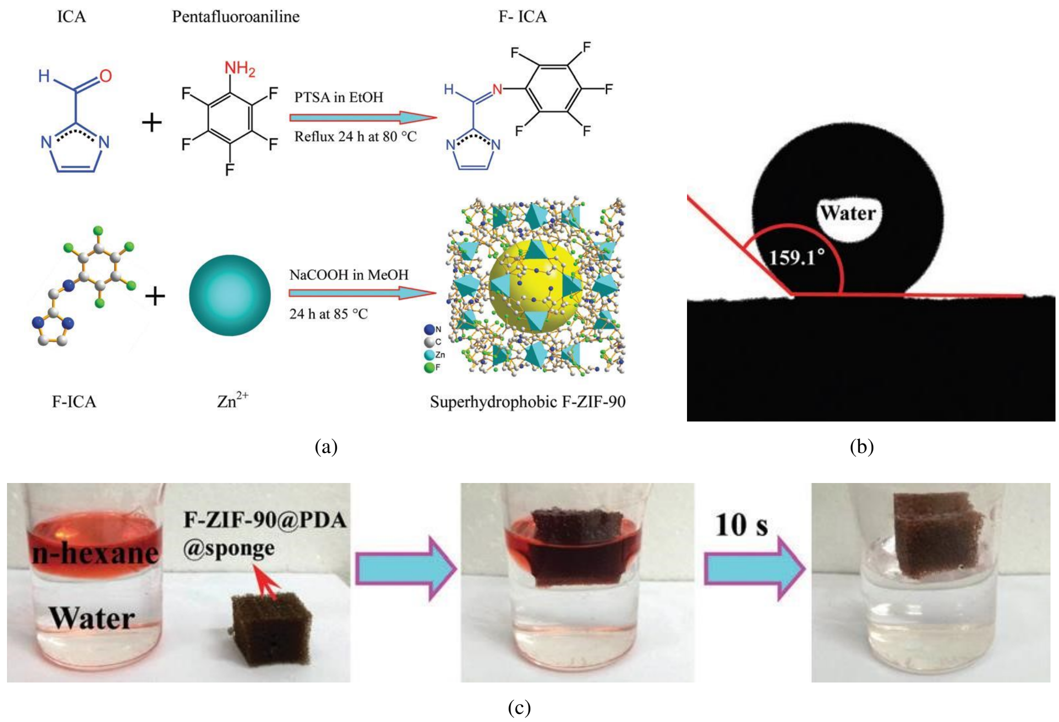

Fig. 10. (a) Scheme of fabrication process, (b) water contact angle, (c) removal of colored n-hexane by using F-ZIF-90@PDA@sponge (Liu and Huang, 2018).

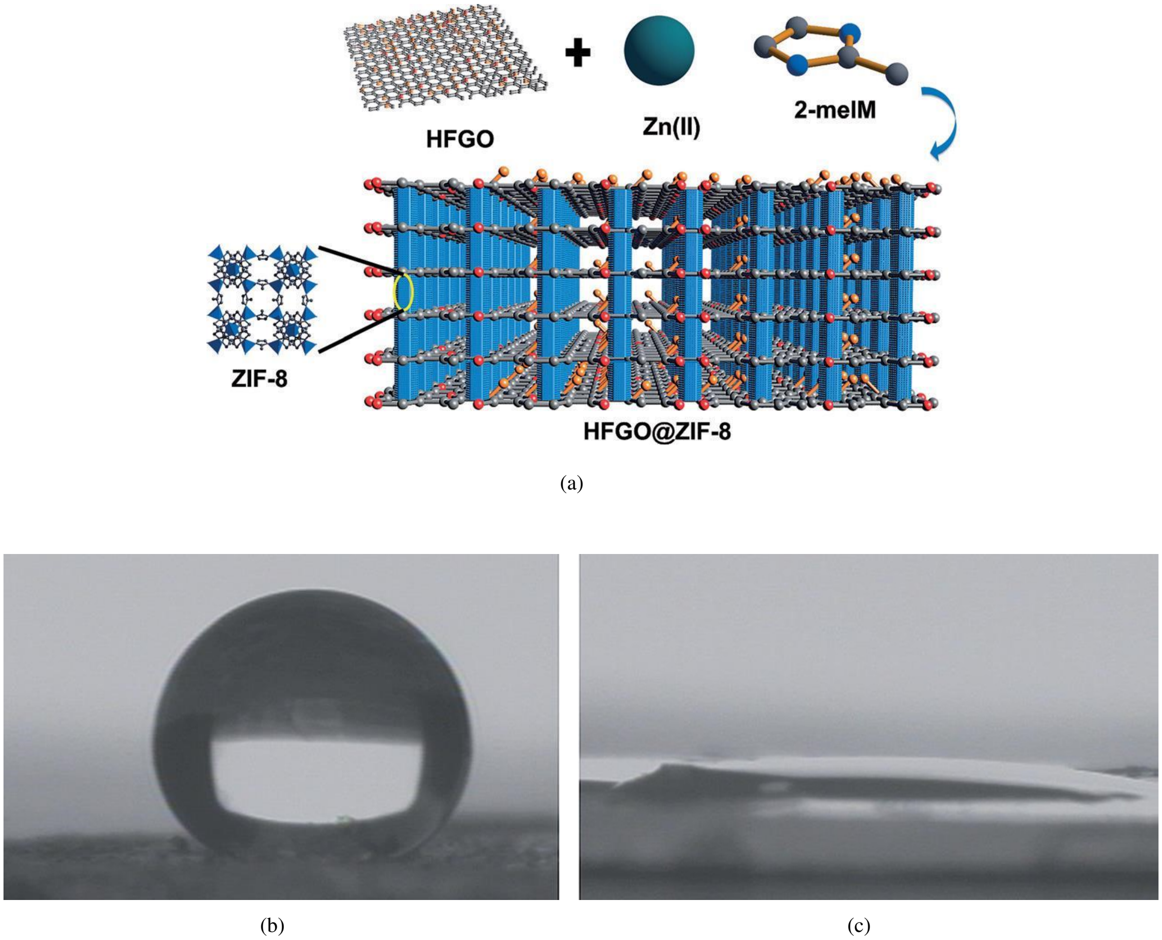

Fig. 11. (a) Schematic of synthesis process, (b) water contact angle, (c) oil contact angle (Jayaramulu et al., 2016).

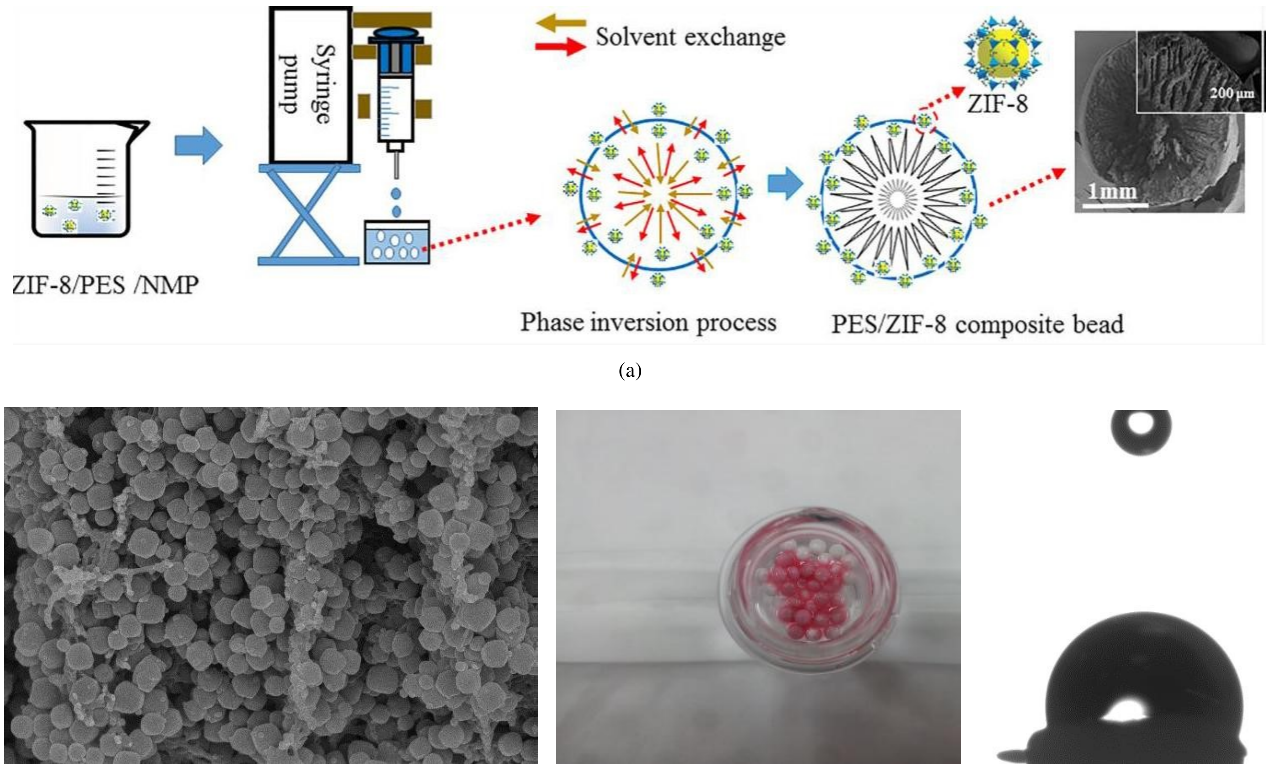

(a)

(b) (c) (d)

Fig. 12. (a) Schematic illustration of formation, (b) Cross sectional SEM image, (c) oil sorption of ZIF-8/PES composite beads, (d) left angle: 100° and right angle: 115° (Abbasi et al., 2017).

carbonization of the melamine foam (25.6 wt% of N) and dip coating of CN foam in the methanol solution having Zn^{2+} and 2-methylimidazole. As a result, the hierarchical porous structure with high hydrophilicity and the water contact angle of 135° prevents water penetration. The maximum absorption content obtained was 58 wt% for chloroform (Kim et al., 2017).

In compositing, ZIF-8 powders incorporated in polylactic acid (PLA) using electrospinning method for membrane application with initial materials of methanol, 2-Methylimidazole, $Zn(NO_3)_2 \cdot 6H_2O$, PLA pellets and CH_2Cl_2 (Dai et al., 2016). Crude oil was absorbed by the PLA/ZIF-8 membrane immediately in comparison with PLA membrane, where oil droplets showed slight stability to the penetration through the membrane due to the smooth surface as shown in Fig. 14a. SEM micrograph revealed that the PLA/ZIF-8 membranes showed improved oleophilic behavior by adding 0.5 wt% ZIF-8 crystals. The mechanical properties increased for tensile strength up to 5.02 MPa rather than pure PLA membrane (Fig. 14b-c) because the flexible structures of ZIF-8 improved the affinity with polymer chains of ligands.

Innovative research was done on ZIF-8 into tea bag as an absorbent for the removal of oil through the synthesis of Zn^{2+} source, 2-methylimidazol, and deionized water in the mixture (Gross et al., 2012; Pan et al., 2015). SEM analysis illustrated the formation of ZIF-8 particles with an average diameter of 238 nm (Fig. 15a) and surface area of 1408 m^2/g extracted from BET date. The prepared sample illustrated strong hydrophobicity with a water contact angle of 142° and reusability by heating process up to twenty cycles (Figs. 15b-c) (Sann et al., 2018).

Xu et al. (2018) studied the micronanofiber membrane of PVDF-g-ZIF-8 by electrospun method including syringe pump, collector, and the high voltage power supply with materials of PVDF, ZnO, N, N-Dimethylacetamide (DMAC), and acetone as solvents along with 2-Methylimidazolate, zinc nitrate hexahydrate, and sodium formate (Fig. 16a). Fig. 16b shows the optimum concentration (8 wt%) of ZIF-8 crystals, lower and higher concentrations of which lead to numerous cavities and agglomeration, respectively. Finally, oleophilic properties of ZIF-crystals increased with a water and toluene contact angle of 158° and 0°, respectively, which revealed the separation yield of 92.93%.

Among the last studies, ZIF-8 has been used more than the other ZIF structures for oil/water separation. Feasibility and high performance of ZIF-8 coverage on melamine sponge with the absorption capacity of 3,800 wt% and on carbon nitride (CN) foam with the capacity of 58 wt% have confirmed the ZIF-8 performance for cleaning up the oil spills (Kim et al., 2017; Lei et al., 2018). It can be considered that pure ZIF-8 powder with very high specific surface area illustrated an absorption capacity in the range of 10 to 150 wt% (Cousin Saint Remi et al., 2011; Jiang et al., 2013). However, the ZIF-8 powders showed a high surface area between 1,000 to 1,700 m^2/g than when it is covered on substrate (Sarker et al., 2017; Sann et al., 2018). Thus, other parameters, namely their

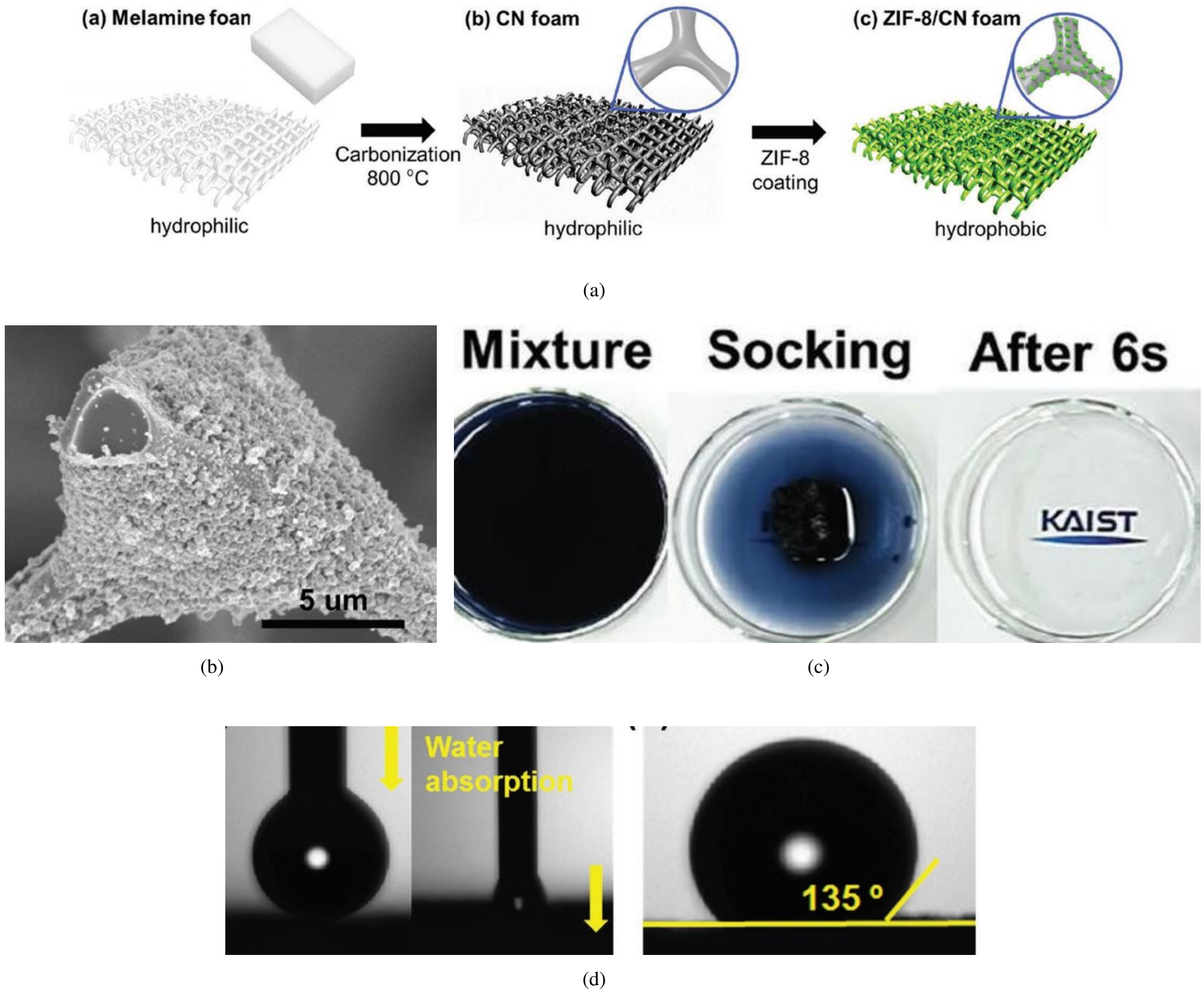

Fig. 13. (a) Schematic representation of the synthesis, (b) SEM micrograph of ZIF-8 attachment, (c) Water contact angle, (d) Images of absorption of ZIF-8/CN foam of ZIF-8/CN foam (Kim et al., 2017).

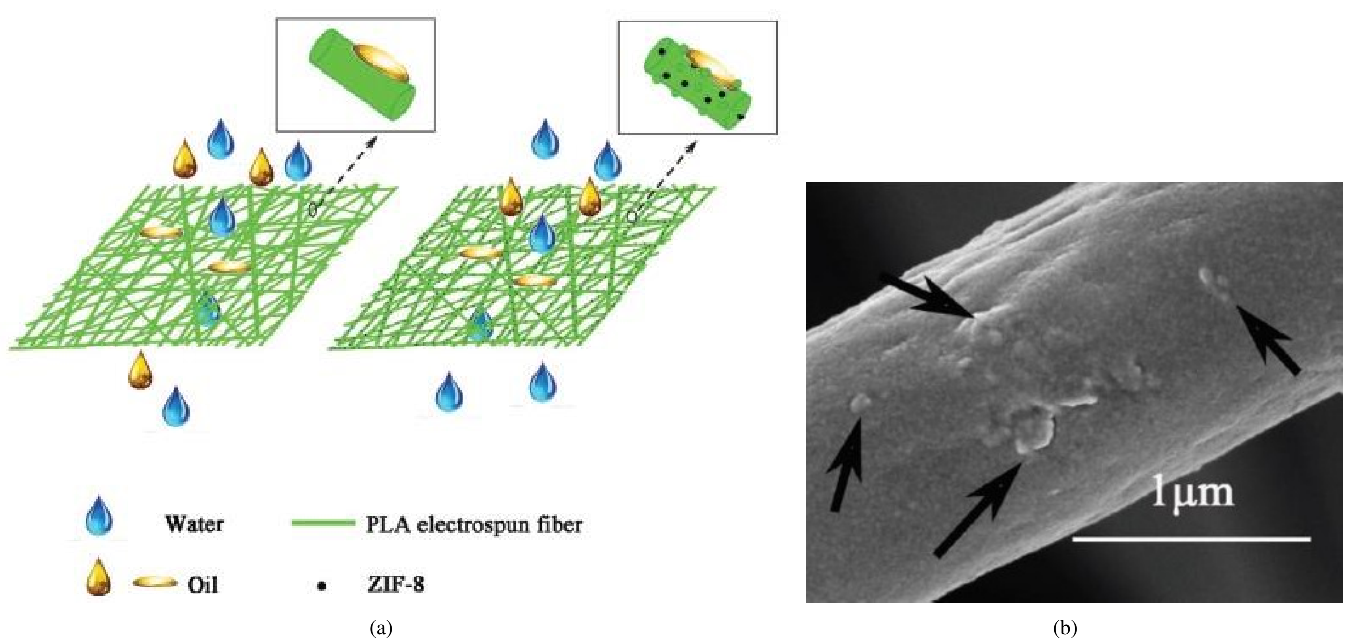

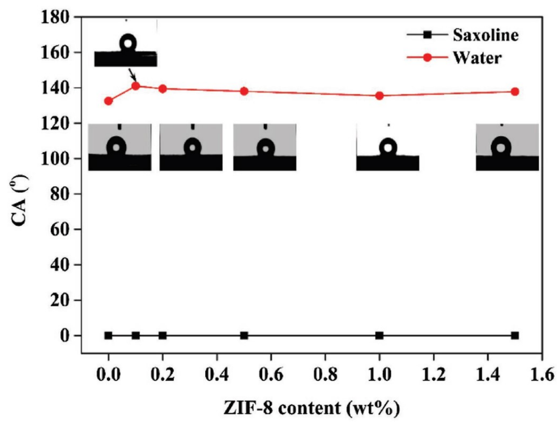

(c)

Fig. 14. (a) Schematic diagrams of oil/water separation, (b) SEM images for PLA/ZIF-8 membranes, (c) Saxoline and water contact angles for pure PLA and PLA/ZIF-8 (Dai et al., 2016).

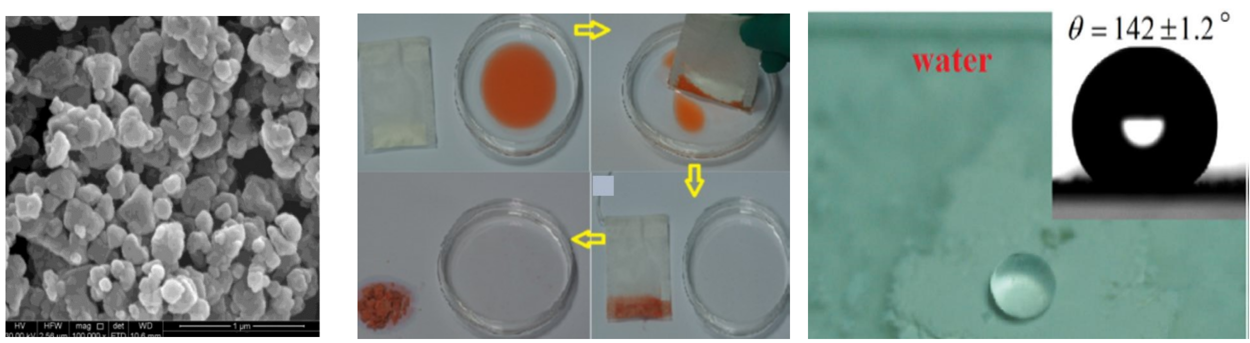

(a) (b) (c)

Fig. 15. (a) SEM images of ZIF-8, (b) Selective removal of oil from oil-water mixtures, (c) Contact angle ZIF-8/Tea bag (Sann et al., 2018).

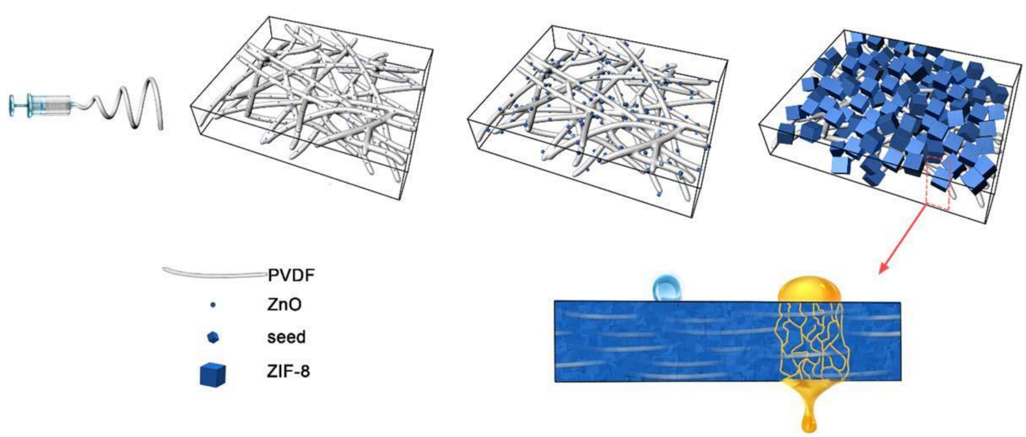

(a) – (b)

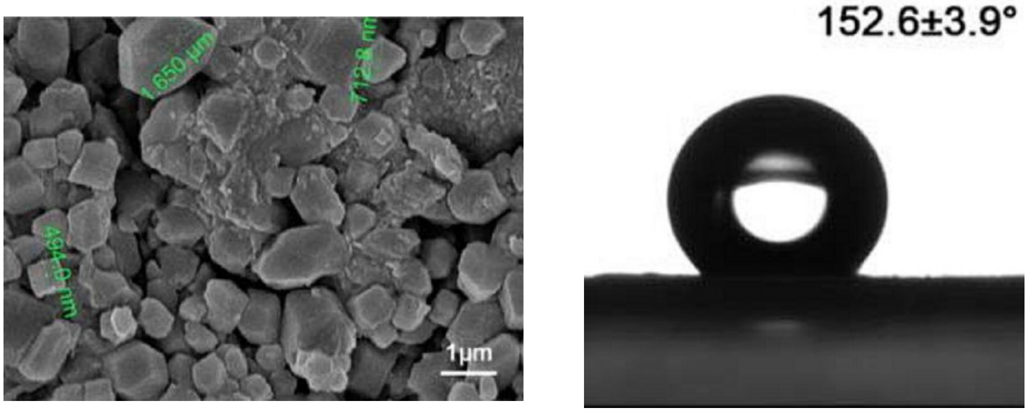

(c) (d)

Fig. 16. (a) Schematic of the membrane fabrication, (b) oil/water separation mechanism, (c) SEM micrograph and (d) Water contact angle of ZIF-8 functionalization membrane (Xu et al., 2018).

secondary porosities due to the connection of ZIF particles on the substrate and capillary effect of inner pores, have shown a very effective role in the absorption capacity. In addition, F-ZIF-90@PDA@sponge rendered the potential of the ZIF-90 for separating capacity up to 4,800 wt% because of having larger cavities than ZIF-8 (Liu and Huang, 2018). The comparison between the studies showed that the absorption of some hydrocarbons with diameters more than ZIF-8 pore size (0.34 nm) was due to the cavities created by the particle bonding on the surface (Bux et al., 2011). In addition, the obtained water contact angle from ZIF coating was introduced as a more important factor for the absorption process. The water contact angle increases with more loading of ZIF particles on the substrate surface and then hydrophobicity increases due to increased roughness. The literature has reported an increase in water contact angle from 60° to 152° superhydrophobicity. These ZIF materials on the template or composition shape are mostly reusable up to 20 cycles.

Use of porous MOF, particularly ZIF crystals, exhibited the obvious advantages of high surface area and hydrophobicity properties as a sorbent. ZIFs are introduced as novel and effective nanostructures for cleaning up oil spills. One of the disadvantages of this study is that the comprehensive comparison with other porous adsorbents, biosorbents, and other methods of oil removal from the water was not investigated. Although this could imitate this study, it could be an opportunity for future research.

6. Summary and conclusions

In this review paper, different crude oil spills in literature were introduced as major pollutants of the seabed water. This study presented a perspective of ZIF structures, synthesis, and applications, factors affecting the sorption, and a description of ZIFs for oil/water separation. Various structures of ZIF crystals were described with the types of imidazole ligands and bonding between N, C, Zn, and H elements. The chemical composition of ligand was introduced as the main determinant of the structure and pore size of ZIF. The performance of ZIF crystals in the recent articles was evaluated as a sorbent for oil/water separation. A holistic view of ZIFs applications in catalysts, biotechnology, energy, etc. was also presented from 2008 to 2019. The most common ZIF structures for crude oil spill cleanup from the water was expressed, where ZIF-8 has been used more than the other structures using 2-methylimidazole as the intact ligand without linking to another agent. The mesoporous diameter of ZIF powders and cavities caused by their interconnecting on the template were expressed as a definite cause of the absorption. Interestingly, it was found that ZIF in various compounds illustrated recoverability up to twenty recycles.

References

Abbasi, Z., Shamsaei, E., Fang, X.Y., et al. Simple fabrication of zeolitic imidazolate framework zif-8/polymer composite beads by phase inversion method for efficient oil sorption. J. Colloid Interface Sci. 2017, 493: 150-161.

Abdi, J., Mahmoodi, N.M., Vossoughi, M., et al. Synthesis of magnetic metal-organic framework nanocomposite (ZIF-8@$Si0_2$@$MnFe_2O_4$) as a novel adsorbent for selective dye removal from multicomponent systems. Microporous Mesoporous Mater. 2019, 273: 177-188.

Adnan, M., Li, K., Wang, J., et al. Hierarchical ZIF-8 toward immobilizing burkholderia cepacia lipase for application in biodiesel preparation. Int. J. Mol. Sci. 2018a, 19(5): E1424.

Adnan, M., Li, K., Xu, L., et al. X-shaped ZIF-8 for immobilization rhizomucor miehei lipase via encapsulation and its application toward biodiesel production. Catalysts 2018b, 8(3): 96.

Ahmed, I., Bhadra, B.N., Lee, H.J., et al. Metal-organic framework-derived carbons: Preparation from ZIF-8 and application in the adsorptive removal of sulfamethoxazole from water. Catal. Today 2018, 301: 90-97.

Andrew Lin, K.Y., Chang, H.A. A zeolitic imidazole framework (ZIF)-sponge composite prepared via a surfactant-assisted dip-coating method. J. Mater. Chem. A 2015, 3(40): 20060-20064.
Arul, P., John, S.A. Organic solvent free in situ growth of flower like co-ZIF microstructures on nickel foam for glucose sensing and supercapacitor applications. Electrochim. Acta 2019, 306: 254-263.
Assfour, B., Leoni, S., Seifert, G. Hydrogen adsorption sites in zeolite imidazolate frameworks ZIF-8 and ZIF-11. J. Phys. Chem. C 2010, 114(31): 13381-13384.
Bagheri, N., Khataee, A., Hassanzadeh, J., et al. Sensitive biosensing of organophosphate pesticides using enzyme mimics of magnetic ZIF-8. Spectrochim. Acta A 2019, 209: 118-125.
Bai, Y., Dong, L., Zhang, C., et al. ZIF-8 filled polydimethylsiloxane membranes for pervaporative separation of n-butanol from aqueous solution. SPE Sci. Technol. 2013, 48(17): 2531-2539.
Banerjee, R., Phan, A., Wang, B., et al. High-throughput synthesis of zeolitic imidazolate frameworks and application to CO_2 capture. Science 2008, 319(5865): 939-943.
Barooah, M., Mandal, B. Synthesis, characterization and CO_2 separation performance of novel PVA/PG/ZIF-8 mixed matrix membrane. J. Memb. Sci. 2019, 572: 198-209.
Bhadra, B.N., Seo, P.W., Khan, N.A., et al. Hydrophobic cobalt-ethylimidazolate frameworks: Phase-pure syntheses and possible application in cleaning of contaminated water. Inorg. Chem. 2016, 55(21): 11362-11371.
Bhardwaj, N., Bhaskarwar, A.N. A review on sorbent devices for oil-spill control. Environ. Pollut. 2018, 243: 1758-1771.
Bhattacharjee, S., Jang, M.S., Kwon, H.J., et al. Zeolitic imidazolate frameworks: Synthesis, functionalization, and catalytic/adsorption applications. Catal. Surv. Asia 2014, 18(4): 101-127.
Bian, Z., Zhang, S., Zhu, X., et al. In situ interfacial growth of zeolitic imidazolate framework (ZIF-8) nanoparticles induced by a graphene oxide pickering emulsion. RSC Adv. 2015, 5(40): 31502-31505.
Bo, S., Ren, W., Lei, C., et al. Flexible and porous cellulose aerogels/zeolitic imidazolate framework (ZIF-8) hybrids for adsorption removal of Cr (IV) from water. J. Solid State Chem. 2018, 262: 135-141.
Bu, X., Lu, Y., Chen, S., et al. Fabrication of porous carbon nitride foams/acrylic resin composites for efficient oil and organic solvents capture. Chem. Eng. J. 2019, 355: 299-308.
Bux, H., Feldhoff, A., Cravillon, J., et al. Oriented zeolitic imidazolate framework-8 membrane with sharp H_2/C_3H_8 molecular sieve separation. Chem. Mater. 2011, 23(8): 2262-2269.
Bux, H., Liang, F., Li, Y., et al. Zeolitic imidazolate framework membrane with molecular sieving properties by microwave-assisted solvothermal synthesis. J. Am. Chem. Soc. 2009, 131(44): 16000-16001.
Chen, E.X., Yang, H., Zhang, J. Zeolitic imidazolate framework as formaldehyde gas sensor. Inorg. Chem. 2014, 53(11): 5411-5413.
Chizallet, C., Lazare, S., Bazer-Bachi, D., et al. Catalysis of transesterification by a nonfunctionalized metalorganic framework: Acido-basicity at the external surface of ZIF-8 probed by ftir and ab initio calculations. J. Am. Chem. Soc. 2010, 132(35): 12365-12377.
Cousin Saint Remi, J., Rmy, T., Van Hunskerken, V., et al. Biobutanol separation with the metal-organic framework ZIF-8. ChemSusChem 2011, 4(8): 1074-1077.
Dai, X., Cao, Y., Shi, X., et al. The pla/zif-8 nanocomposite membranes: The diameter and surface roughness adjustment by ZIF-8 nanoparticles, high wettability, improved mechanical property, and efficient oil/water separation. Adv. Mater. Interfaces 2016, 3(24): 1600725.
Dejam, M. Dispersion in non-newtonian fluid flows in a conduit with porous walls. Chem. Eng. Sci. 2018, 189: 296-310.
Dejam, M. Derivation of dispersion coefficient in an electro-osmotic flow of a viscoelastic fluid through a porous-walled microchannel. Chem. Eng. Sci. 2019a, 204: 298-309.
Dejam, M. Hydrodynamic dispersion due to a variety of flow velocity profiles in a porous-walled microfluidic channel. Int. J. Heat Mass Transf. 2019b, 136: 87-98.
Dejam, M., Hassanzadeh, H., Chen, Z. Shear dispersion in combined pressure-driven and electro-osmotic flows in a capillary tube with a porous wall. AIChE J. 2015a, 61(11): 3981-3995.
Dejam, M., Hassanzadeh, H., Chen, Z. Shear dispersion in combined pressure-driven and electro-osmotic flows in a channel with porous walls. Chem. Eng. Sci. 2015b, 137: 205-215.
Esfahanian, M., Ghasemzadeh, M.A., Razavian, S.M.H. Synthesis, identification and application of the novel metal-organic framework Fe_3O_4@PAA@ZIF-8 for the drug delivery of ciprofloxacin and investigation of antibacterial activity. Artif. Cells Nanomed. Biotechnol. 2019, 47(1): 2024-2030.
Feng, X.J., Jiang, L. Design and creation of superwetting/antiwetting surfaces. Adv. Mater. 2006, 18(23): 3063-3078.
Fingas, M. Chapter 14-spill-treating Agents, in Oil Spill Science and Technology. Boston, USA, Gulf Professional Publishing, 2011.
Fu, Q., Ansari, F., Zhou, Q., et al. Wood nanotechnology for strong, mesoporous, and hydrophobic biocomposites for selective separation of oil/water mixtures. ACS Nano 2018, 12(3): 2222-2230.
Gao, M.L., Zhao, S.Y., Chen, Z.Y., et al. Superhydrophobic/-superoleophilic mof composites for oil-water separation. Inorg. Chem. 2019, 58(4): 2261-2264.
Gao, X., Xu, L.P., Xue, Z., et al. Dual-scaled porous nitrocellulose membranes with underwater superoleophobicity for highly efficient oil/water separation. Adv. Mater. 2014, 26(11): 1771-1775.
Ge, J., Ye, Y.D., Yao, H.B., et al. Pumping through porous hydrophobic/oleophilic materials: An alternative technology for oil spill remediation. Angew. Chem. Int. Ed. 2014, 53(14): 3612-3616.

Go, Y., Lee, J.H., Shamsudin, I.K., et al. Microporous ZIF-7 membranes prepared by in-situ growth method for hydrogen separation. Int. J. Hydrogen Energy 2016, 41(24): 10366-10373.

Gore, P.M., Purushothaman, A., Naebe, M., et al. Nanotechnology for Oil-water Separation, in Advanced Research in Nanosciences for Water Technology. Cham, Springer International Publishing, 2019.

Gross, A.F., Sherman, E., Vajo, J.J. Aqueous room temperature synthesis of cobalt and zinc sodalite zeolitic imidizolate frameworks. Dalton T. 2012, 41(18): 5458-5460.

Guan, Y., Cheng, F., Pan, Z. Superwetting polymeric three dimensional (3d) porous materials for oil/water separation: A review. Polymers 2019, 11(5): 806.

Guo, Y., Wang, X., Hu, P., et al. ZIF-8 coated polyvinylidenefluoride (pvdf) hollow fiber for highly efficient separation of small dye molecules. Appl. Mater. Today 2016, 5: 103-110.

Hou, X.J., Li, H. Unraveling the high uptake and selectivity of CO_2 in the zeolitic imidazolate frameworks ZIF-68 and ZIF-69. J. Phys. Chem. C 2010, 114(32): 13501-13508.

Huang, A., Caro, J. Covalent post-functionalization of zeolitic imidazolate framework ZIF-90 membrane for enhanced hydrogen selectivity. Angew. Chem. Int. Ed. 2011, 50(21): 4979-4982.

Huang, A., Chen, Y., Wang, N., et al. A highly permeable and selective zeolitic imidazolate framework ZIF-95 membrane for H_2/CO_2 separation. Chem. Commun. 2012a, 48(89): 10981-10983.

Huang, A., Dou, W., Caro, J. Steam-stable zeolitic imidazolate framework ZIF-90 membrane with hydrogen selectivity through covalent functionalization. J. Am. Chem. Soc. 2010, 132(44): 15562-15564.

Huang, A., Liu, Q., Wang, N., et al. Bicontinuous zeolitic imidazolate framework ZIF-8@GO membrane with enhanced hydrogen selectivity. J. Am. Chem. Soc. 2014, 136(42): 14686-14689.

Huang, A., Wang, N., Kong, C., et al. Organosilica-functionalized zeolitic imidazolate framework ZIF-90 membrane with high gas-separation performance. Angew. Chem. Int. Ed. 2012b, 51(42): 10551-10555.

Huang, G., Zhang, F., Du, X., et al. Metal organic frameworks route to in situ insertion of multiwalled carbon nanotubes in Co_3O_4 polyhedra as anode materials for lithium-ion batteries. ACS Nano 2015, 9(2): 1592-1599.

Hurd, J.A., Vaidhyanathan, R., Thangadurai, V., et al. Anhydrous proton conduction at 150 °C in a crystalline metal-organic framework. Nat. Chem. 2009, 1: 705.

International Tanker Owners Pollution Federation (ITOPF). 2019.

Isanejad, M., Arzani, M., Mahdavi, H.R., et al. Novel amine modification of ZIF-8 for improving simultaneous removal of cationic dyes from aqueous solutions using supported liquid membrane. J. Mol. Liq. 2017, 225: 800-809.

Jayaramulu, K., Datta, K.K.R., Rsler, C., et al. Biomimetic superhydrophobic/superoleophilic highly fluorinated graphene oxide and ZIF-8 composites for oil-water separation. Angew. Chem. Int. Ed. 2016, 55(3): 1178-1182.

Jayaramulu, K., Geyer, F., Petr, M., et al. Shape controlled hierarchical porous hydrophobic/oleophilic metal-organic nanofibrous gel composites for oil adsorption. Adv. Mater. 2017, 29(12): 1605307.

Jiang, H.L., Liu, B., Akita, T., et al. Au@ZIF-8: Co oxidation over gold nanoparticles deposited to metalorganic framework. J. Am. Chem. Soc. 2009, 131(32): 11302-11303.

Jiang, J.Q., Yang, C.X., Yan, X.P. Zeolitic imidazolate framework-8 for fast adsorption and removal of benzotriazoles from aqueous solution. ACS Appl. Mater. Interfaces 2013, 5(19): 9837-9842.

Jiang, P., Hu, Y., Li, G. Biocompatible Au@Ag nanorod@ZIF-8 core-shell nanoparticles for surface-enhanced raman scattering imaging and drug delivery. Talanta 2019a, 200: 212-217.

Jiang, Z., Wang, Y., Sun, L., et al. Dual atp and ph responsive ZIF-90 nanosystem with favorable biocompatibility and facile post-modification improves therapeutic outcomes of triple negative breast cancer in vivo. Biomaterials 2019b, 197: 41-50.

Jin, H., Li, Y., Liu, X., et al. Recovery of hmf from aqueous solution by zeolitic imidazolate frameworks. Chem. Eng. Sci. 2015, 124: 170-178.

Kharisov, B.I., Dias, H.V.R., Kharissova, O.V. Nanotechnology-based remediation of petroleum impurities from water. J. Pet. Sci. Eng. 2014, 122: 705-718.

Khay, I., Chaplais, G., Nouali, H., et al. Water intrusion-extrusion experiments in ZIF-8: Impacts of the shape and particle size on the energetic performances. RSC Adv. 2015, 5(40): 31514-31518.

Khosravi, M., Azizian, S. Synthesis of a novel highly oleophilic and highly hydrophobic sponge for rapid oil spill cleanup. ACS Appl. Mater. Interfaces 2015, 7(45): 25326-25333.

Kim, D., Kim, D.W., Buyukcakir, O., et al. Highly hydrophobic ZIF-8/Carbon nitride foam with hierarchical porosity for oil capture and chemical fixation of CO_2. Adv. Funct. Mater. 2017, 27(23): 1700706.

Kou, Z., Dejam, M. Dispersion due to combined pressure-driven and electro-osmotic flows in a channel surrounded by a permeable porous medium. Phys. Fluids 2019, 31(5): 056603.

Kumar, R., Raut, D., Ahmad, I., et al. Functionality preservation with enhanced mechanical integrity in the nanocomposites of the metal-organic framework, zif-8, with bn nanosheets. Mater. Horiz. 2014, 1(5): 513-517.

Kumar, V., Vellingiri, K., Kukkar, D., et al. Recent advances and opportunities in the treatment of hydrocarbons and oils: Metal-organic frameworks-based approaches. Crit. Rev. Environ. Sci. Technol. 2019, 49(7): 587-654.

Kuruppathparambil, R.R., Jose, T., Babu, R., et al. A room temperature synthesizable and environmental friendly heterogeneous ZIF-67 catalyst for the solvent less and co-catalyst free synthesis of cyclic carbonates. Appl. Catal. B 2016, 182: 562-569.

Kvenvolden, K.A., Cooper, C.K. Natural seepage of crude oil into the marine environment. Geo-Mar. Lett. 2003, 23(3): 140-146.

Lahann, J. Environmental nanotechnology: Nanomaterials clean up. Nat. Nanotechnol. 2008, 3: 320-321.

Lee, C.H., Tiwari, B., Zhang, D., et al. Water purification: Oil-water separation by nanotechnology and environmental concerns. Environ. Sci. Nano 2017, 4(3): 514-525.

Lei, W., Portehault, D., Liu, D., et al. Porous boron nitride nanosheets for effective water cleaning. Nat. Commun. 2013, 4: 1777.

Lei, Z., Deng, Y., Wang, C. Multiphase surface growth of hydrophobic ZIF-8 on melamine sponge for excellent oil/water separation and effective catalysis in a knoevenagel reaction. J. Mater. Chem. A 2018, 6(7): 3258-3263.

Li, C.R., Hai, J., Fan, L., et al. Amplified colorimetric detection of Ag^+ based on Ag^+-triggered peroxidase-like catalytic activity of ZIF-8/GO nanosheets. Sens. Actuators B Chem. 2019a, 284: 213-219.

Li, D., Guo, Z. Metal-organic framework superhydrophobic coating on kevlar fabric with efficient drag reduction and wear resistance. Appl. Surf. Sci. 2018, 443: 548-557.

Li, F., Zheng, K., Zhang, H., et al. Nanoscale hierarchically porous metal-organic frameworks: Facile synthesis, mechanism research, and application. ACS Sustain. Chem. Eng. 2019b, 7(13): 11080-11087

Li, J., Li, D., Yang, Y., et al. A prewetting induced underwater superoleophobic or underoil (super) hydrophobic waste potato residue-coated mesh for selective efficient oil/water separation. Green Chem. 2016, 18(2): 541-549.

Li, J., Lin, J., Xu, X., et al. Porous boron nitride with a high surface area: Hydrogen storage and water treatment. Nanotechnology 2013, 24(15): 155603.

Li, K., Olson, D.H., Seidel, J., et al. Zeolitic imidazolate frameworks for kinetic separation of propane and propene. J. Am. Chem. Soc. 2009, 131(30): 10368-10369.

Li, Q., Guo, J., Zhu, H., et al. Space-confined synthesis of ZIF-67 nanoparticles in hollow carbon nanospheres for CO_2 adsorption. Small 2019c, 15(8): 1804874.

Li, Y., Zhang, H., Fan, M., et al. A robust salt-tolerant superoleophobic aerogel inspired by seaweed for efficient oil-water separation in marine environments. Phys. Chem. Chem. Phys. 2016, 18(36): 25394-25400.

Liang, H.W., Guan, Q.F., Chen, L.F., et al. Macroscopic-scale template synthesis of robust carbonaceous nanofiber hydrogels and aerogels and their applications. Angew. Chem. Int. Ed. 2012, 51(21): 5101-5105.

Liang, K., Coghlan, C.J., Bell, S.G., et al. Enzyme encapsulation in zeolitic imidazolate frameworks: A comparison between controlled co-precipitation and biomimetic mineralisation. Chem. Commun. 2016a, 52(3): 473-476.

Liang, K., Richardson, J.J., Cui, J., et al. Metal-organic framework coatings as cytoprotective exoskeletons for living cells. Adv. Mater. 2016b, 28(36): 7910-7914.

Lin, J., Shang, Y., Ding, B., et al. Nanoporous polystyrene fibers for oil spill cleanup. Mar. Pollut. Bull. 2012, 64(2): 347-352.

Lin, K.Y.A., Chen, Y.C., Phattarapattamawong, S. Efficient demulsification of oil-in-water emulsions using a zeolitic imidazolate framework: Adsorptive removal of oil droplets from water. J. Colloid Interface Sci. 2016, 478: 97-106.

Liu, C., Huang, A. One-step synthesis of the superhydrophobic zeolitic imidazolate framework F-ZIF-90 for efficient removal of oil. New J. Chem. 2018, 42(4): 2372-2375.

Liu, J. Construction of Nafion/Hb/Au/ZIF-8/CILE and its application as electrochemical sensor for determination of bromate and nitrite. Int. J. Electrochem. Sci. 2019, 14: 1310-1317.

Liu, X., Li, Y., Ban, Y., et al. Improvement of hydrothermal stability of zeolitic imidazolate frameworks. Chem. Commun. 2013, 49(80): 9140-9142.

Liu, Y., Hu, E., Khan, E.A., et al. Synthesis and characterization of ZIF-69 membranes and separation for CO_2/CO mixture. J. Memb. Sci. 2010, 353(1): 36-40.

Lively, R.P., Dose, M.E., Thompson, J.A., et al. Ethanol and water adsorption in methanol-derived ZIF-71. Chem. Commun. 2011, 47(30): 8667-8669.

Lu, G., Hupp, J.T. Metalorganic frameworks as sensors: A ZIF-8 based fabryprot device as a selective sensor for chemical vapors and gases. J. Am. Chem. Soc. 2010, 132(23): 7832-7833.

Mao, J., Ge, M., Huang, J., et al. Constructing multifunctional MOF@rGO hydro-/aerogels by the self-assembly process for customized water remediation. J. Mater. Chem. A 2017, 5(23): 11873-11881.

Miao, Z., Yang, F., Luan, Y., et al. Synthesis of Fe_3O_4@P4VP@ZIF-8 core-shell microspheres and their application in a knoevenagel condensation reaction. J. Solid State Chem. 2017, 256: 27-32.

Michel, J. Chapter 37-1991 Gulf War Oil Spill, in Oil spill science and technology. Boston, USA, Gulf Professional Publishing, 2011.

Moggach, S.A., Bennett, T.D., Cheetham, A.K. The effect of pressure on ZIF-8: Increasing pore size with pressure and the formation of a high-pressure phase at 1.47 gpa. Angew. Chem. 2009, 121(38): 7221-7223.

Mokhatab, S., Fresky, M.A., Islam, M.R. Applications of nanotechnology in oil and gas E&P. J. Pet. Technol. 2006, 58(4): 48-51.

Mondal, S.S., Hovestadt, M., Dey, S., et al. Synthesis of a partially fluorinated ZIF-8 analog for ethane/ethene separation. CrystEngComm 2017, 19(39): 5882-5891.

Nabeel Rashin, M., Kutty, R.G., Hemalatha, J. Novel coconut oil based magnetite nanofluid as an ecofriendly oil spill remover. Ind. Eng. Chem. Res. 2014, 53(40): 15725-15730.

Nakano, T., Nozue, Y. Orbital degeneracy and magnetic properties of potassium clusters incorporated into nanoporous crystals of zeolite A. J. Comput. Methods Sci. Eng. 2007, 7: 443-462.

Nasir, A.M., Md Nordin, N.A.H., Goh, P.S., et al. Application of two-dimensional leaf-shaped zeolitic imidazolate framework (2d ZIF-l) as arsenite adsorbent: Kinetic, isotherm and mechanism. J. Mol. Liq. 2018, 250: 269-

277.
Pan, Y., Li, H., Zhang, X.X., et al. Large-scale synthesis of ZIF-67 and highly efficient carbon capture using a ZIF-67/glycol-2-methylimidazole slurry. Chem. Eng. Sci. 2015, 137: 504-514.
Parajuli, D., Sue, K., Takahashi, A., et al. Adsorption of ng l1-level arsenic by zif-8 nanoparticles: Application to the monitoring of environmental water. RSC Adv. 2018, 8(63): 36360-36368.
Pendergast, M.M., Hoek, E.M.V. A review of water treatment membrane nanotechnologies. Energy Environ. Sci. 2011, 4(6): 1946-1971.
Phan, A., Doonan, C.J., Uribe-Romo, F.J., et al. Synthesis, structure, and carbon dioxide capture properties of zeolitic imidazolate frameworks. Accounts Chem. Res. 2010, 43(1): 58-67.
Qian, J., Sun, F., Qin, L. Hydrothermal synthesis of zeolitic imidazolate framework-67 (ZIF-67) nanocrystals. Mater. Lett. 2012, 82: 220-223.
Rankin, R.B., Liu, J., Kulkarni, A.D., et al. Adsorption and diffusion of light gases in ZIF-68 and ZIF-70: A simulation study. J. Phys. Chem. C 2009, 113(39): 16906-16914.
Ren, G., Li, Z., Yang, W., et al. Zno@zif-8 core-shell microspheres for improved ethanol gas sensing. Sens. Actuators B Chem. 2019, 284: 421-427.
Rettig, S.J., Storr, A., Summers, D.A., et al. Iron (ii) 2-methylimidazolate and copper (ii) 1,2,4-triazolate complexes: Systems exhibiting long-range ferromagnetic ordering at low temperatures. Can. J. Chem. 1999, 77(4): 425-433.
Sánchez, J., Zornoza, B., Mayoral, Á., et al. Beyond the H_2/CO_2 upper bound: One-step crystallization and separation of nano-sized ZIF-11 by centrifugation and its application in mixed matrix membranes. J. Mater. Chem. A 2015, 3(12): 6549-6556.
Sánchez, J., Zornoza, B., Tllez, C., et al. On the chemical filler-polymer interaction of nano- and micro-sized ZIF-11 in pbi mixed matrix membranes and their application for H_2/CO_2 separation. J. Mater. Chem. A 2016, 4(37): 14334-14341.
Sann, E.E., Pan, Y., Gao, Z., et al. Highly hydrophobic ZIF-8 particles and application for oil-water separation. Sep. Purif. Technol. 2018, 206: 186-191.
Sarker, M., Bhadra, B.N., Seo, P.W., et al. Adsorption of benzotriazole and benzimidazole from water over a co-based metal azolate framework maf-5 (CO). J. Hazard. Mater. 2017, 324: 131-138.
Seoane, B., Zamaro, J.M., Tllez, C., et al. Insight into the crystal synthesis, activation and application of ZIF-20. RSC Adv. 2011, 1(5): 917-922.
Shamsaei, E., Lin, X., Low, Z.X., et al. Aqueous phase synthesis of ZIF-8 membrane with controllable location on an asymmetrically porous polymer substrate. ACS Appl. Mater. Interfaces 2016, 8(9): 6236-6244.
Shang, Y., Si, Y., Raza, A., et al. An in situ polymerization approach for the synthesis of superhydrophobic and superoleophilic nanofibrous membranes for oil-water separation. Nanoscale 2012, 4(24): 7847-7854.
Shekhah, O., Fu, L., Sougrat, R., et al. Successful implementation of the stepwise layer-by-layer growth of mof thin films on confined surfaces: Mesoporous silica foam as a first case study. Chem. Commun. 2012, 48(93): 11434-11436.
Shi, L., Chen, K., Du, R., et al. Scalable seashell-based chemical vapor deposition growth of three-dimensional graphene foams for oil-water separation. J. Am. Chem. Soc. 2016, 138(20): 6360-6363.
Shin, J.H., Heo, J.H., Jeon, S., et al. Bio-inspired hollow pdms sponge for enhanced oil-water separation. J. Hazard. Mater. 2019, 365: 494-501.
Si, Y., Fu, Q., Wang, X., et al. Superelastic and superhydrophobic nanofiber-assembled cellular aerogels for effective separation of oil/water emulsions. ACS Nano 2015, 9(4): 3791-3799.
Singh, V., Purkait, M.K., Das, C. Cross-flow microfiltration of industrial oily wastewater: Experimental and theoretical consideration. SPE. Sci. Technol. 2011, 46(8): 1213-1223.
Su, P., Xiao, H., Zhao, J., et al. Nitrogen-doped carbon nanotubes derived from Zn-Fe-ZIF nanospheres and their application as efficient oxygen reduction electrocatalysts with in situ generated iron species. Chem. Sci. 2013, 4(7): 2941-2946.
Sun, C.Y., Qin, C., Wang, X.L., et al. Zeolitic imidazolate framework-8 as efficient ph-sensitive drug delivery vehicle. Dalton T. 2012, 41(23): 6906-6909.
Taylor, J.M., Mah, R.K., Moudrakovski, I.L., et al. Facile proton conduction via ordered water molecules in a phosphonate metalorganic framework. J. Am. Chem. Soc. 2010, 132(40): 14055-14057.
The Guardian Newspaper. 2011.
Thornton, A.W., Dubbeldam, D., Liu, M.S., et al. Feasibility of zeolitic imidazolate framework membranes for clean energy applications. Energy Environ. Sci. 2012, 5(6): 7637-7646.
Tian, D., Zhang, X., Tian, Y., et al. Photo-induced water-oil separation based on switchable superhydrophobicity-superhydrophilicity and underwater superoleophobicity of the aligned zno nanorod array-coated mesh films. J. Mater. Chem. 2012, 22(37): 19652-19657.
Tian, Y.Q., Cai, C.X., Ji, Y., et al. $[Co_5(im)_{10}*2MB]_\infty$: A metal-organic open-framework with zeolite-like topology. Angew. Chem. Int. Ed. 2002, 41(8): 1384-1386.
Tsai, C.W., Langner, E.H.G. The effect of synthesis temperature on the particle size of nano-ZIF-8. Microporous Mesoporous Mater. 2016, 221: 8-13.
Valadez Snchez, E.P., Gliemann, H., Haas-Santo, K., et al. ZIF-8 surmof membranes synthesized by au-assisted liquid phase epitaxy for application in gas separation. Chem. Ing. Tech. 2016, 88(11): 1798-1805.
Venna, S.R., Carreon, M.A. Highly permeable zeolite imidazolate framework-8 membranes for CO_2/CH_4 separation. J. Am. Chem. Soc. 2010, 132(1): 76-78.
Wang, G., He, Y., Wang, H., et al. A cellulose sponge with robust superhydrophilicity and under-water superoleo-

phobicity for highly effective oil/water separation. Green Chem. 2015a, 17(5): 3093-3099.

Wang, H., Zhou, H., Niu, H., et al. Dual-layer superamphiphobic/superhydrophobic-oleophilic nanofibrous membranes with unidirectional oil-transport ability and strengthened oil-water separation performance. Adv. Mater. Interfaces 2015b, 2(4): 1400506.

Wang, Q., Wang, X., Shi, C. Ldh nanoflower lantern derived from zif-67 and its application for adsorptive removal of organics from water. Ind. Eng. Chem. Res. 2018a, 57(37): 12478-12484.

Wang, S., Hou, Y., Lin, S., et al. Water oxidation electrocatalysis by a zeolitic imidazolate framework. Nanoscale 2014, 6(17): 9930-9934.

Wang, Y., Feng, Y., Yao, J. Construction of hydrophobic alginate-based foams induced by zirconium ions for oil and organic solvent cleanup. J. Colloid Interface Sci. 2019, 533: 182-189.

Wang, Z., Tang, X., Wang, X., et al. Near-infrared light-induced dissociation of zeolitic imidazole framework-8 (ZIF-8) with encapsulated cus nanoparticles and their application as a therapeutic nanoplatform. Chem. Commun. 2016, 52(82): 12210-12213.

Wang, Z., Yu, G., Xia, J., et al. One-step synthesis of a methylene blue@ZIF-8-reduced graphene oxide nanocomposite and its application to electrochemical sensing of rutin. Microchim. Acta 2018b, 185(5): 279.

Wee, L.H., Janssens, N., Sree, S.P., et al. Local transformation of ZIF-8 powders and coatings into zno nanorods for photocatalytic application. Nanoscale 2014, 6(4): 2056-2060.

Wenzel, R.N. Resistance of solid surfaces to wetting by water. Ind. Eng. Chem. 1936, 28(8): 988-994.

Wu, C., Liu, Q., Chen, R., et al. Fabrication of ZIF-8@SiO_2 micro/nano hierarchical superhydrophobic surface on az31 magnesium alloy with impressive corrosion resistance and abrasion resistance. ACS Appl. Mater. Interfaces 2017a, 9(12): 11106-11115.

Wu, D., Fang, L., Qin, Y., et al. Oil sorbents with high sorption capacity, oil/water selectivity and reusability for oil spill cleanup. Mar. Pollut. Bull. 2014a, 84(1): 263-267.

Wu, J., Wang, N., Wang, L., et al. Electrospun porous structure fibrous film with high oil adsorption capacity. ACS Appl. Mater. Interfaces 2012, 4(6): 3207-3212.

Wu, L., Li, L., Li, B., et al. Magnetic, durable, and superhydrophobic polyurethane@Fe_3O_4@SiO_2@fluoropolymer sponges for selective oil absorption and Oil/Water separation. ACS Appl. Mater. Interfaces 2015, 7(8): 4936-4946.

Wu, R., Qian, X., Rui, X., et al. Zeolitic imidazolate framework 67-derived high symmetric porous CO_3O_4 hollow dodecahedra with highly enhanced lithium storage capability. Small 2014b, 10(10): 1932-1938.

Wu, T., Feng, X., Elsaidi, S.K., et al. Zeolitic imidazolate framework-8 (ZIF-8) membranes for Kr/Xe separation. Ind. Eng. Chem. Res. 2017b, 56(6): 1682-1686.

Xia, W., Mahmood, A., Zou, R., et al. Metal-organic frameworks and their derived nanostructures for electrochemical energy storage and conversion. Energy Environ. Sci. 2015, 8(7): 1837-1866.

Xue, C.H., Ji, P.T., Zhang, P., et al. Fabrication of superhydrophobic and superoleophilic textiles for oil-water separation. Appl. Surf. Sci. 2013, 284: 464-471.

Xu, S., Ren, L.F., Zhou, Q., et al. Facile ZIF-8 functionalized hierarchical micronanofiber membrane for high-efficiency separation of water-in-oil emulsions. J. Appl. Polym. Sci. 2018, 135(27): 46462.

Xu, X., Dong, F., Yang, X., et al. Preparation and characterization of cellulose grafted with epoxidized soybean oil aerogels for oil-absorbing materials. J. Agric. Food Chem. 2019a, 67(2): 637-643.

Xu, Z., Wang, J., Li, H., et al. Coating sponge with multifunctional and porous metal-organic framework for oil spill remediation. Chem. Eng. J. 2019b, 370: 1181-1187.

Yaghi, O.M., Li, H. Hydrothermal synthesis of a metal-organic framework containing large rectangular channels. J. Am. Chem. Soc. 1995, 117(41): 10401-10402.

Yang, H., He, X.W., Wang, F., et al. Doping copper into ZIF-67 for enhancing gas uptake capacity and visible-light-driven photocatalytic degradation of organic dye. J. Mater. Chem. 2012, 22(41): 21849-21851.

Yang, Q., Lu, R., Ren, S., et al. Three dimensional reduced graphene oxide/ZIF-67 aerogel: Effective removal cationic and anionic dyes from water. Chem. Eng. J. 2018a, 348: 202-211.

Yang, Q., Lu, R., Ren, S., et al. Magnetic beads embedded in poly (sodium-p-styrenesulfonate) and ZIF-67: Removal of nitrophenol from water. J. Solid State Chem. 2018b, 265: 200-207.

Yang, T., Chung, T.S. High performance ZIF-8/pbi nanocomposite membranes for high temperature hydrogen separation consisting of carbon monoxide and water vapor. Int. J. Hydrogen Energy 2013, 38(1): 229-239.

Yin, H., Khosravi, A., OConnor, L., et al. Effect of ZIF-71 particle size on free-standing ZIF-71/pdms composite membrane performances for ethanol and 1-butanol removal from water through pervaporation. Ind. Eng. Chem. Res. 2017, 56(32): 9167-9176.

Yong, J., Huo, J., Chen, F., et al. Oil/water separation based on natural materials with super-wettability: Recent advances. Phys. Chem. Chem. Phys. 2018, 20(39): 25140-25163.

Yoon, S.M., Park, J.H., Grzybowski, B.A. Large-area, freestanding mof films of planar, curvilinear, or micropatterned topographies. Angew. Chem. Int. Ed. 2017, 56(1): 127-132.

Yuan, J., Hung, W.S., Zhu, H., et al. Fabrication of ZIF-300 membrane and its application for efficient removal of heavy metal ions from wastewater. J. Memb. Sci. 2019, 572: 20-27.

Yu, L.Q., Yan, X.P. Covalent bonding of zeolitic imidazolate framework-90 to functionalized silica fibers for solid-phase microextraction. Chem. Commun. 2013, 49(21): 2142-2144.

Yu, Y., Chen, H., Liu, Y., et al. Superhydrophobic and superoleophilic porous boron nitride nanosheet/polyvinylidene fluoride composite material for oil-polluted water cleanup. Adv. Mater. Interfaces 2015, 2(1): 1400267.

Zakzeski, J., Dbczak, A., Bruijnincx, P.C.A., et al. Catalytic oxidation of aromatic oxygenates by the heterogeneous catalyst Co-ZIF-9. Appl. Catal. A Gen. 2011, 394(1): 79-85.

Zhang, E., Cheng, Z., Lv, T., et al. Anti-corrosive hierarchical structured copper mesh film with superhydrophilicity and underwater low adhesive superoleophobicity for highly efficient oil-water separation. J. Mater. Chem. A 2015, 3(25): 13411-13417.

Zhang, F., Zhang, W.B., Shi, Z., et al. Nanowire-haired inorganic membranes with superhydrophilicity and underwater ultralow adhesive superoleophobicity for high-efficiency oil/water separation. Adv. Mater. 2013a, 25(30): 4192-4198.

Zhang, G., Zhang, J., Su, P., et al. Non-activation mof arrays as a coating layer to fabricate a stable superhydrophobic micro/nano flower-like architecture. Chem. Commun. 2017, 53(59): 8340-8343.

Zhang, H., Zhao, M., Lin, Y.S. Stability of ZIF-8 in water under ambient conditions. Microporous Mesoporous Mater. 2019a, 279: 201-210.

Zhang, J., Wang, Y., Xiao, K., et al. N-doped hierarchically porous carbon derived from heterogeneous core-shell ZIF-l(Zn)@ZIF-67 for supercapacitor application. New J. Chem. 2018, 42(9): 6719-6726.

Zhang, K., Lively, R.P., Dose, M.E., et al. Alcohol and water adsorption in zeolitic imidazolate frameworks. Chem. Commun. 2013b, 49(31): 3245-3247.

Zhang, K., Lively, R.P., Zhang, C., et al. Investigating the intrinsic ethanol/water separation capability of ZIF-8: An adsorption and diffusion study. J. Phys. Chem. C 2013c, 117(14): 7214-7225.

Zhang, T., Yuan, D., Guo, Q., et al. Preparation of a renewable biomass carbon aerogel reinforced with sisal for oil spillage clean-up: Inspired by green leaves to green tofu. Food Bioprod. Process. 2019b, 114: 154-162.

Zhang, T., Zhang, X., Yan, X., et al. Synthesis of Fe_3O_4@ZIF-8 magnetic core-shell microspheres and their potential application in a capillary microreactor. Chem. Eng. J. 2013d, 228: 398-404.

Zheng, B., Wang, L.L., Du, L., et al. Diffusion as a function of guest molecule length and functionalization in flexible metal-organic frameworks. Mater. Horiz. 2016, 3(4): 355-361.

Zhong, G., Liu, D., Zhang, J. The application of ZIF-67 and its derivatives: Adsorption, separation, electrochemistry and catalysts. J. Mater. Chem. A 2018, 6(5): 1887-1899.

Zhu, H., Yang, X., Cranston, E.D., et al. Flexible and porous nanocellulose aerogels with high loadings of metal-organic-framework particles for separations applications. Adv. Mater. 2016, 28(35): 7652-7657.

Zhu, H., Zhang, Q., Li, B.G., et al. Engineering elastic ZIF-8-Sponges for oil-water separation. Adv. Mater. Interfaces 2017, 4(20): 1700560.